University of Copenhagen

Bachelor Thesis

Quantum Phase Transition in an Ion Trap

Author:
Kasper Ejdal Lund, *mjb253*

Supervisor:
Anders S. Sørensen

June 11, 2014

Abstract

English

This thesis considers the interaction between N ions confined in an ion trap and a set of laser fields, described by the Dicke model. The Dicke Hamiltonian for the two different models, used by the research group at the *University of Innsbruck* (the Quantum Optics and Spectroscopy group) and the Quantum Optics group at the *National Institute of Science and Technology* in Boulder, Colorado, respectively. The Innsbruck model uses an effective two-level system, while the Boulder model uses a Δ-system, which is reduced to a two-level system by eliminating the excited level adiabatically.
This thesis shows that the system undergoes a phase transition at a critical value of the Lamb-Dicke parameter η, where the system goes from the ground state into a state characterized by super radiance, where the atomic ensemble spontaneously emits radiation with intensity proportional to N^2. The existence of the phase transition is shown from a mean-field description of the Dicke model and from the Holstein-Primakoff representation of the model in the thermodynamic limit $N \to \infty$. This representation enables a physical interpretation of, and a detailed description of, the phase transition.
A direct numerical diagonalization of the ground state of the Dicke Hamiltonian have been carried out to test the behaviour of a finite number of ions. This diagonalization also indicates that the system needs to prepared in such a way that the interaction with the laser fields excite more oscillations in the center-of-mass mode than in the atomic spin.
The possibility of measuring the phase transition has also been discussed by numerically solving the time-dependent Schrödinger equation for various linear models of the Lamb-Dicke parameter. It is shown that the Lamb-Dicke parameter needs to be adiabatically driven to properly measure the phase transition and that the deviation from the phase transition decreases as the Lamb-Dicke parameter is driven more slowly. Lastly the universality of the phase transition is discussed.

Dansk

Denne bacheloropgave omhandler interaktionen mellem N ioner i en ionfælde og en række lasere, beskrevet ved hjælp af Dicke-modellen. Dicke Hamiltonen er blevet opstillet for to forskellige modeller, der bliver brugt af henholdsvis Quantum Optics and Spectroscopy group fra *University of Innsbruck* og kvanteoptik-gruppen fra *National Institute of Science and Technology* i Boulder, Colorado. Innsbruck-modellen bruger et to-niveau atom, mens at Boulder-modellen bruger et $\Delta-$system, der reduceres til et to-niveau system ved at eliminere the tredje niveau adiabatisk.
Denne opgave viser, at der findes en faseovergang i system ved en kritisk værdi af Lamb-Dicke parameteren η for systemets grundtilstand. Denne faseovergang går fra grundtilstanden til en tilstand, hvor det atomare ensemble er karakteriseret ved begrebet "super-radiance", hvor ensemblet udsender spontant emitteret stråling med en intensitet proportional til N^2. Faseovergangens eksistens bevises gennem en middelfelts-beskrivelse til nulte og første orden, blandt andet ved hjælp af Holstein-Primakoff repræsentationen af modellen i den thermodynamiske grænse $N \to \infty$. Denne repræsentation muliggør desuden en fysisk fortolkning af faseovergangen.
Grundtilstanden for Dicke Hamiltonen er blevet diagonaliseret numerisk for at teste om hvordan antallet af ioner i fælden påvirker faseovergangen. Diagonaliseringen viser også, at systemet skal forberedes sådan, at interaktionen danner flere ekscitationer i oscillationen i ionernes massemidtpunkt end i det atomare spin.
Den tidsafhængige Schrödingerligning er blevet løst numerisk for at undersøge muligheden for at måle faseovergangen i et eksperiment. Dette er gjort for forskellige lineære modeller for Lamb-Dicke parameteren. I den forbindelse vises det, at Lamb-Dicke parameteren skal køres adiabatisk langsomt i tid , od det vises desuden, at afvigelsen fra grundtilstanden samtidig bliver mindre. Universaliteten af faseovergangen diskuteres til slut.

Contents

1 Introduction

Phase transitions are well described in various physical systems; examples include the ordering of bosons in the ground state in Bose-Einstein condensation or the transition between a ferromagnetic system to a paramagnetic system as the temperature is increased above the Cure temperature. A similar phase transition can be found in the Dicke model describing the interaction between a number of lasers and an atomic ensemble.

This thesis expands upon the procedure outlined in [5] and examines the conditions for the phase transition in the Dicke model through two different ion-laser interactions, used by the experimental quantum optics groups at the University of Innsbruck and at the National Institute for Science and Technology in Boulder, respectively. These are referred to as Innsbruck and Boulder, Colorado, respectively, in the rest of the thesis. The interaction Hamiltonian is derived for both models and the existence of the phase transition is demonstrated through a mean-field description of the Hamiltonian. The aim of this thesis is to demonstrate the importance of an adiabatic evolution of the appropriate parameters in order to induce the phase transition, e.g. a rapid increase in, say, the Lamb-Dicke parameter $\eta(t)$ will not yield a phase transition, but an adiabatic evolution will.

The thesis also aims to present a simple model for the evolution of $\eta(t)$ that can be used in an experiment to observe the phase transition. It is assumed that the Lamb-Dicke parameter evolves linearly in time and present different slopes - those that permit the phase transition and those that do not.
This thesis in organized in the following sections:

- Section 2 introduces the formalism used to describe an atomic ensemble and a quantized light field. It also introduces the quantum mechanical angular momentum formalism used in this thesis and outlines the general procedure for changing to the interaction picture. The two models are also introduced and the general form of the interaction Hamiltonian for each are presented.
- Section 3 outlines the change to the interaction picture for the two models. This section only describes the unique features in the mathematical derivation so most of the detailed calculations have been omitted from this section. These can be found in Appendix (A). Note that the application of standard quantum optics methods, primarily the application of the Baker-Hausdorf lemma, have been omitted completely from this thesis, and it is assumed that the reader is familiar with these methods.
  The existence of phase transition is also shown and the critical value for η is derived through a zeroth-order mean-field description of the Hamiltonian and a first-order description is made using the Holstein-Primakoff representation of angular momentum operators. This enables a physical interpretation of the phase transition.
- Section 4 discusses the phase transition in detail, in three different ways:
  - The ground state of the Hamiltonian have been diagonalized for varying ratios of the strength of the spin and the cavity oscillator. This part examines the phase transition's dependence on the number N of ions in the ion trap, as well as the dependence on the strengths of the spin and the oscillator.
  - The time dependent Schrödinger equation have been numerically solved for various ratios of the strength of the spin and the oscillator, as well for different models for the time-evolution fo the Lamb-Dicke parameter $\eta(t)$. This part examines the adiabatic evolution of $\eta(t)$ and aims to find a model for $\eta(t)$ that permits the existence of the phase transition.
  - The universality of the phase transition is shown, meaning that the phase transition exist for any number of ions confined in the trap. This is done by finding the optimal model for a given set of parameters. This is done for varying numbers of ions and it is shown that the relationship between the second derivative of the z-component of the spin and the optimal slope is essentially the same, regardless of the number of ions in the trap.
- Section 5 concludes on the results, primarily those from section 4, and provides an outlook for further study.

We set $\hbar = 1$ throughout the thesis, which causes the unit of energy and frequency to coincide.

2 Formalism

2.1 The Interaction-Free System

The interaction-free ion-laser system can be split up in two separate parts: An ion part described by the atomic Hamiltonian $\hat{H}_a$ and the vector space $\mathcal{V}_a$, and an electromagnetic part, describing the quantized electric field using the Hamiltonian $\hat{H}_{EM}$ and the vector space $\mathcal{V}_{EM}$. The total vector space of the system is written as the product space $\mathcal{V} = \mathcal{V}_a \otimes \mathcal{V}_{EM}$. The two vector spaces, as well as the corresponding Hamiltonians, are defined in the following sections.

2.1.1 The Atomic Ensemble

We will in general be considering an ensemble of N atoms confined in the trap. The ions used in the Innsbruck model have two energy levels for the n^{th} ion: $|g\rangle_n$ and $|e\rangle_n$, while the Boulder model uses a three level system, comprised of a hyperfine split ground state: $|1\rangle_n$ and $|2\rangle_n$, and an excited level $|e\rangle_n$. This model is, however, approximated as a two-level system by adiabatically eliminating the excited state $|e\rangle_n$.
The Hamiltonian for the atomic ensemble in the Innsbruck model can be written as the sum of the individual atomic Hamiltonians $\hat{H}_a = \sum_n \hat{H}_a^{(n)}$. The n^{th} atomic Hamiltonian can be written in a diagonal form in terms of the energies of the ground state and the excited state, $E_g^{(n)}$ and $E_e^{(n)}$, respectively:

$$\hat{H}_a^n = E_g^{(n)} |g\rangle_n \langle g|_n + E_e^{(n)} |e\rangle_n \langle e|_n \tag{1}$$

The atomic Hamiltonian in the Boulder model is written in the same manner, where the E_g term is replaced by a sum over the two ground state energies: $E_g^{(n)} |g\rangle_n \langle g|_n = E_0^{(n)} |0\rangle_n \langle 0|_n + E_1^{(n)} |1\rangle_n \langle 1|_n$.

2.1.2 Angular Momentum Operator Formalism

Both systems can be described in terms of spin-$\frac{1}{2}$ angular momentum operators, provided that the excited state in the Boulder model is adiabatically eliminated. These operators are, for the n^{th} atom with the $z-$axis as the quantization axis, defined in terms of the Pauli spin matrices as:

$$\hat{\sigma}_{z,n} = (|1\rangle_n \langle 1|_n - |0\rangle_n \langle 0|_n), \quad \hat{\sigma}_{+,n} = |1\rangle_n \langle 0|_n ; \quad \hat{\sigma}_{-,n} = |0\rangle_n \langle 1|_n \tag{2}$$

$$\hat{\sigma}_{x,n} = \frac{1}{2}(\hat{\sigma}_{+,n} + \hat{\sigma}_{-,n}) ; \quad \hat{\sigma}_{y,n} = \frac{i}{2}(\hat{\sigma}_{-,n} - \hat{\sigma}_{+,n}) \tag{3}$$

These operators $\hat{\sigma}_{i,n}$ $(i = x, y, z)$ obey the standard angular momentum commutation relations $[\hat{\sigma}_{i,m}, \hat{\sigma}_{j,n}] = \sum_k i\epsilon_{ijk}\hat{\sigma}_{k,m}\delta_{m,n}$. The collective angular momentum operators $\hat{J}_i, i = (x, y, z, \pm)$, that acts on the entire system, can be defined by $\hat{J}_i = \sum_n \hat{\sigma}_{i,n}$.
These operators also obey the angular momentum commutation relations

$$\left[\hat{J}_i, \hat{J}_j\right] = \sum_{n,m} [\hat{\sigma}_{i,n}, \hat{\sigma}_{j,m}] = \sum_{n,m}\sum_k i\epsilon_{ijk}\hat{\sigma}_{k,n}\delta_{n,m} = \sum_k i\epsilon_{ijk}\hat{J}_k \tag{4}$$

$\hat{J}_z$ is an eigenfunction of the product state $|S\rangle = |s_1, s_1\rangle |s_2, m_2\rangle ... |s_N, m_N\rangle$, such that

$$\hat{J}_z |S\rangle = \left[\sum_{n=1}^{N} m_n\right] |S\rangle$$

It is assumed that the system have the largest possible spin $J \equiv \sum_{n=1}^{N} s_n = \frac{N}{2}$, since all ions can be described as a spin$\frac{1}{2}$ system. The eigenvalues for the raising and lowering operators for the n^{th} ion are given by: $S_{n,\pm} |s, m_n\rangle = \sqrt{(s \mp m_n)(s + 1 \pm m_n)} |s, m_n \pm 1\rangle$.

This formulation allows us to write the atomic Hamiltonian from equation (1) in a more helpful manner. The zero-energy point is chosen to lie directly between the ground state and the excited state, such that $E_1^{(n)} = \frac{\omega_0}{2}$ and $E_0^{(n)} = -\frac{\omega_0}{2}$:

$$\hat{H}_a = \sum_{n=1}^{N} E_1^{(n)} |1\rangle_n \langle 1|_n - E_0^{(n)} |0\rangle_n \langle 0|_n = \frac{\omega_0}{2} \sum_{n=1}^{N} \frac{1}{2} \left(|1\rangle_n \langle 1|_n - |0\rangle_n \langle 0|_n \right) = \frac{\omega_0}{2} \sum_{n=1}^{N} \hat{\sigma}_{z,n} = \frac{\omega_0}{2} \hat{J}_z \quad (5)$$

2.1.3 The Laser Field and the Ion Trap

The quantized cavity field is replaced with a quantized vibrational motion of the center-of-mass (abbreviated as COM) of the trapped ions. The Hamiltonian for an electromagnetic wave with frequency ω can be written as a harmonic oscillator:

$$\hat{H}_{EM} = \sum_{k=1}^{N} \frac{1}{2} \left[p^2 + C \left(x_{k+1} - x_k \right) \right] \quad (6)$$

where the last term describes the coupling between two ions, with the force constant C. This Hamiltonian can be greatly simplified by changing to phonon coordinates, i.e. by replacing the displacement $\hat{x}_j$ of the j^{th} ion from its equilibrium position by a linear combination of N coordinates $\hat{q}_j$ by setting $\hat{x}_j = \sum_{l=1}^{N} b_j^l \hat{q}_l$, where b_j^l obeys the orthogonality conditions $\sum_{j=1}^{N} b_j^l b_j^{l'} = \delta_{l,l'}$ and $\sum_{l=1}^{N} b_j^l b_{j'}^l = \delta_{j,j'}$. A similar change for the momentum coordinates is made: $p_j \to P_k$, such that $[q_k, P_{k'}] = i\delta_{k,k'}$. It can be shown that the transformed Hamiltonian is (the details can be found in appendix (C)):

$$\hat{H}_{EM} = \frac{1}{2} \sum_{j=1}^{N} \left[P_j P_{-j} + \omega_j^2 q_j q_{-j} \right] \quad (7)$$

where ω_j is the frequency of the j^{th} phonon coordinate. This allows us to write $\hat{x}$ in terms of the annihilation and creation operators ($\hat{a}_l$ and $\hat{a}_l^\dagger$) of the l^{th} mode by:

$$\hat{q}_l = \sum_{l=1}^{N} \sqrt{\frac{1}{2\nu_l m}} \left(\hat{a}_l + \hat{a}_l^\dagger \right) \quad (8)$$

using standard methods in quantum optics found in any introductory quantum optics textbooks (see for instance reference [4]), with the Hamiltonian

$$\hat{H}_{EM} = \sum_{l}^{N} \nu_l \left(\hat{a}_l^\dagger \hat{a}_l + \frac{1}{2} \right) \quad (9)$$

The laser field of frequency ω_L is described by:

$$E^-(\hat{x}, t) = \sum_{j=1}^{N} \frac{E_0}{2} \exp\left[i \left(\omega_{L,j} t - k_L \hat{x} + \phi \right) \right] + C.C.$$

where C.C. is the complex conjugate, E_0 is the amplitude of the field, $k_L = 2\pi/\lambda_L$ is the component of the wave vector of the field along the trap axis, and ϕ is a phase. The field can be written in terms of $\hat{a}_l$ and $\hat{a}_l^\dagger$ using equation (8):

$$E^-(\hat{x}, t) = \sum_{j=1}^{N} \frac{E_0}{2} e^{i(\omega_{L,j} t + \phi)} e^{-i \sum_{l=1}^{N} \eta_l \left(\hat{a}_l + \hat{a}_l^\dagger \right)} \quad (10)$$

where $\eta_l \equiv k_L \sqrt{\frac{1}{2\nu_l m}}$ is the Lamb-Dicke parameter, given by $\eta_{j,n} = \eta_n \frac{\sqrt{N} b_j}{\sqrt{\nu'/\nu}}$, $\eta_n = k_n \sqrt{\frac{1}{2m\nu N}}$, where m is the mass of the ion. The subscript n refers to the n^{th} laser, if there is more than one. These operators

create and annihilate quanta of vibrational motion and operate on the so-called Fock-space, where the natural basis for the l^{th} mode is the occupation number n_l, defined as the eigenvalue of the number operator $\hat{n}_l = \hat{a}_l^\dagger \hat{a}_l$, such that: $\hat{n}_l |n_l\rangle = n_l |n_l\rangle$, where n_l is the number of excitations in the oscillator in the l^{th} mode. The total basis is then the product state $|\hat{n}\rangle = \prod_l \otimes |\hat{n}_l\rangle$

Equations (5) and (9) can be combined to give the interaction-free Hamiltonian of the form

$$\hat{H}_0 = \frac{\omega_0}{2}\hat{J}_z + \sum_{l=1}^{N} \nu_l \hat{a}_l^\dagger \hat{a}_l \tag{11}$$

where the zero-point energy has been dropped.

2.2 The Dipole Interaction

The interaction between the ensemble of ions and an electric field is well described by the dipole interaction, characterized by the Hamiltonian:

$$\hat{H}_I = -D^- \hat{\sigma}_- \hat{E}^- (\hat{x}, t) + H.C. \tag{12}$$

where H.C. is the hermitian conjugate, $\hat{E}^-(\hat{x}, t)$ is the negative frequency part of the laser field and D^- is the corresponding dipole moment for the $|g\rangle \leftrightarrow |e\rangle$ transition. We also have D^+ for the positive frequency term. The exact form of the Hamiltonian depends on the system and are defined for the two models in section (2.3).

It is convenient to change to the interaction picture with respect to a suitable Hamiltonian $\hat{H}_c$ by using the unitary operator $\hat{U}_0 = \exp\left[-i\hat{H}_c t\right]$ by:

$$\begin{aligned} \tilde{H}_I &= \hat{U}_0^\dagger \hat{H} \hat{U}_0 - i\hat{U}^\dagger \frac{\partial \hat{U}_0}{\partial t} \\ &= \hat{U}_0^\dagger \hat{H}_I \hat{U}_0 + \hat{U}_0^\dagger \hat{H}_0 \hat{U}_0 - \hat{U}_0^\dagger \hat{H}_c \hat{U}_0 \end{aligned} \tag{13}$$

where it has been used that $\frac{\partial \hat{U}_0}{\partial t} = -i\hat{H}_c \hat{U}_0$ from which it follows that $i\hat{U}_0^\dagger \frac{\partial \hat{U}_0}{\partial t} = \hat{U}_0^\dagger \hat{H}_c \hat{U}_0$. It is often convenient to choose $\hat{H}_c = \hat{H}_0$, such that $\tilde{H}_I = \hat{U}_0^\dagger \hat{H}_I \hat{U}_0$, but other choices may be viable.

2.3 The Ion-Laser Models

2.3.1 The Innsbruck Model

The research group in Innsbruck uses a qubit comprised of the metastable states $|g\rangle \equiv S_{1/2}\,(m = 1/2)$ and $|e\rangle \equiv D_{5/2}\,(m = 3/2)$ of the isotope $^{40}Ca^+$. The transition interacts with a bichromatic laser field with frequencies $\omega_{1,2} = \omega_0 \pm \delta$, where ω_0 is the qubit transition frequency and δ is close the l^{th} vibrational mode frequency. Further details about the experimental set up can be found at [1]. This model is modified slightly: the lasers are further detuned by a small frequency ϵ from ω_0, which is necessary to induce the phase transition. The energy diagram for the model is shown in figure (1).

The interaction-free Hamiltonian for the j^{th} ion is:

$$\hat{H}_{0,j} = \sum_{l=1}^{N} \nu_l \hat{a}_l^\dagger \hat{a}_l + \frac{\omega_0}{2}\hat{\sigma}_{z,j} \tag{14}$$

The laser fields are characterized by

$$\begin{aligned} E_1 &= \frac{E_0}{2} \exp\left[-i\overline{k}_1 \hat{\overline{r}}\right] \exp\left[i\left(\omega_1 t + \phi_1\right)\right] + C.C. \\ E_2 &= \frac{E_0}{2} \exp\left[-i\overline{k}_2 \hat{\overline{r}}\right] \exp\left[i\left(\omega_2 t + \phi_2\right)\right] + C.C. \end{aligned}$$

where $\overline{k}$ is the wave vector associated with each field and ϕ_i are the phases of each laser. $\hat{\overline{r}}$ is the position of the ion, which oscillates about the equilibrium position r_0 with the small displacement $\delta\hat{\overline{r}}$.

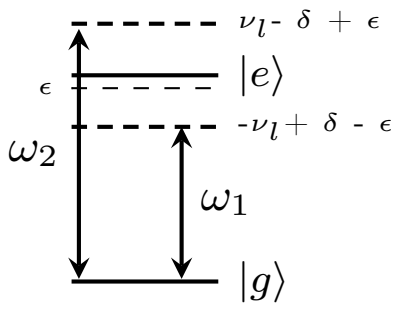

Figure 1: Energy diagram for the Innsbruck Model

The equilibrium term only contributes a phase factor ϕ_r, while the displacement can be given in terms of the annihilation and creation operators for the l^{th} mode by:

$$\overline{k}\delta\hat{\overline{r}} = \sum_{l=1}^{N} k_l \sqrt{\frac{1}{2m\nu_l}} \left(\hat{a}_l + \hat{a}_l^\dagger\right) = \sum_{l=1}^{N} \eta_l \left(\hat{a}_l + \hat{a}_l^\dagger\right)$$

The total phase is described by: $\Phi_i = \phi_i + r_0$ and it is assumed that both lasers have the same phase Φ. The interaction-Hamiltonian is given by:

$$\hat{H}_I = \left[D_1^- \frac{E_0}{2} e^{i\omega_1 t} e^{-i\sum_{l=1}^{N} \eta_{1,l}\left(\hat{a}_l + \hat{a}_l^\dagger\right)} e^{i\Phi_1} + D_2^- \frac{E_0}{2} e^{i\omega_2 t} e^{-i\sum_{l=1}^{N} \eta_{2,l}\left(\hat{a}_l + \hat{a}_l^\dagger\right)} e^{i\Phi_2} \right] |e\rangle\langle g| + H.C. \tag{15}$$

where D_i^- is the dipole moment for the transition between the two level for the i^{th} laser. It is advantageous to tune the laser phase to $\Phi = \Phi' + \pi/2$, such that $e^{i\Phi} = ie^{\Phi'}$. It is then possible, with no loss of generality, to absorb the phases into the state $ie^{i\Phi'}|e\rangle\langle g| = i|\tilde{e}\rangle\langle g| = i\tilde{\sigma}_-$, where the tildes are omitted in the rest of the thesis. The Rabi frequency is defined as $\Omega_n = \frac{D_n^- E_0}{2}$. The interaction Hamiltonian then takes the form:

$$\hat{H}_I = i\hat{\sigma}_- \left[\Omega_1 e^{i\omega_1 t} e^{-i\sum_{l=1}^{N} \eta_{1,l}\left(\hat{a}_l + \hat{a}_l^\dagger\right)} + \Omega_2 e^{i\omega_2 t} e^{-i\sum_{l=1}^{N} \eta_{2,l}\left(\hat{a}_l + \hat{a}_l^\dagger\right)} \right] + H.C. \tag{16}$$

2.3.2 The Boulder Model

The model used by the research group in Boulder is composed of two $^9Be^+$ hyperfine ground states ($|0\rangle \equiv |F = 2, m_F = -2\rangle$ and $|1\rangle \equiv |F = 1, m_F = -1\rangle$) and an excited state $|e\rangle$. Only the motion corresponding to the resonant COM mode with frequency ν is considered, for simplicity. Further details about the experimental set up can be found at [2]. The energy diagram for a single ion is shown in figure(2).
The system interacts with two bichromatic lasers with frequencies ω_1, ω_3 for the first laser and ω_2, ω_4 for the second laser. The beam directions are at right angle to each other and the direction in the wavevector difference $\Delta\overline{k} = \overline{k}_1 - \overline{k}_2$ coincides with the trap axis. The laser fields interact with an ion located at the equilibrium position $\hat{\overline{r}}_0$ and are given by

$$E_1(\overline{r}, t) = \frac{E_0}{2} \exp\left[i\left(\overline{k}_1\hat{\overline{r}} - \omega_i t + \phi\right)\right] + C.C. \tag{17}$$

$$E_2(\overline{r}, t) = \frac{E_0}{2} \exp\left[i\left(\overline{k}_2\hat{\overline{r}} - \omega_j t + \phi\right)\right] + C.C. \tag{18}$$

where, $k_{1,2}$ and $\omega_{i,j}$ is the wavevector and frequency for each laser (with $i = 1, 3$ and $j = 2, 4$). It is assumed that the lasers have the same phase ϕ and both lasers are detuned by $\Delta \approx 2\pi \cdot 82$GHz from the 2s $^2S_{1/2} \rightarrow$ 2p $^2P_{1/2}$ electric dipole transition with wavelength $\lambda = 313$nm.

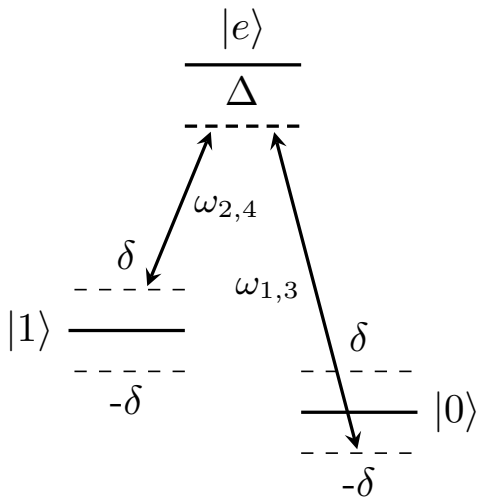

Figure 2: Energy diagram for the Boulder Model

We look at the situation with two ions confined in the trap. The first ion is located at $\hat{\bar{r}}_1$ while the second is located at $\hat{\bar{r}}_2$. The position of the i^{th} ion can be written as a deviation $\delta\hat{\bar{r}}_i$ from the equilibrium position $\hat{\bar{r}}_{0,i}$, such that $\hat{\bar{r}}_i = \hat{\bar{r}}_{0,i} + \delta\hat{\bar{r}}_i$. The deviation is the same for the two ions when they are in the COM mode $\delta\hat{\bar{r}}_1 = \delta\hat{\bar{r}}_2 \equiv \delta\hat{\bar{r}}$ and the distance between the ions is: $\hat{\bar{d}} = \hat{\bar{r}}_2 - \hat{\bar{r}}_1 = \hat{\bar{r}}_{0,1} - \hat{\bar{r}}_{0,2}$.
The laser phase is absorbed into ttheir respective states, as in the Innsbruck model: $e^{i\phi}|0\rangle\langle e| = |\tilde{0}\rangle\langle e|$ and $e^{i\phi}|1\rangle\langle e| = |\tilde{1}\rangle\langle e|$. We need to keep the contribution to the phase from the equilibrium positions, $e^{i\hat{\bar{r}}_{0,i}}$, due to interference effects from the lasers.
The displacement can be given in terms of the annihilation and creation operators:

$$\bar{k}\delta\hat{\bar{r}} = k\sqrt{\frac{1}{2m\nu}}\left(\hat{a} + \hat{a}^\dagger\right) = \eta\left(\hat{a} + \hat{a}^\dagger\right)$$

The interaction Hamiltonian $\hat{H}_I$ is given by:

$$\left.\begin{aligned}\hat{H}_I = |0\rangle\langle e|\left(e^{i\bar{k}_1\hat{\bar{r}}_1}\alpha_{10}e^{-i\omega_1 t} + e^{i\bar{k}_2\hat{\bar{r}}_1}\alpha_{20}e^{-i\omega_2 t} + e^{i\bar{k}_1\hat{\bar{r}}_2}\alpha_{10}e^{-i\omega_1 t} + e^{i\bar{k}_2\hat{\bar{r}}_2}\alpha_{20}e^{-i\omega_2 t}\right) + H.C. \\ + |1\rangle\langle e|\left(e^{i\bar{k}_1\hat{\bar{r}}_1}\alpha_{11}e^{-i\omega_3 t} + e^{i\bar{k}_2\hat{\bar{r}}_1}\alpha_{21}e^{-i\omega_4 t} + e^{i\bar{k}_1\hat{\bar{r}}_2}\alpha_{11}e^{-i\omega_3 t} + e^{i\bar{k}_2\hat{\bar{r}}_2}\alpha_{21}e^{-i\omega_4 t}\right) + H.C. + \Delta|e\rangle\langle e|\end{aligned}\right\} \tag{19}$$

where $\alpha_{ij} = \Omega_i\alpha'_{i,j}$ with $i = 1, 2$ and $j = |0\rangle, |1\rangle$, where Ω_i is defined as in section (2.3.1). This term describes the strength of the dipole transition for the j^{th} ground state interacting with the i^{th} laser by the product of the Rabi frequency for the transition Ω_i and a "strength"-factor α'_{ij}. This factor describes possible changes in the strength of the Rabi frequency due to effects from atomic physics. It it assumed that these terms are real numbers, but they can be complex numbers in a more general treatment. There are certain restriction to combinations of these factors, where the important combinations are $\alpha_{10}\alpha_{20} = -\alpha_{11}\alpha_{21}$ and $\alpha_{12}\alpha_{20} = \alpha_{10}\alpha_{21}$. The other combinations are irrelevant in this thesis, as they do not enter into $\hat{H}_I$ or, alternatively, they appear in terms that are approximately zero in the rotating wave approximation (RWA) applied in section (3).

3 Changing to the Interaction Picture

3.1 The Innsbruck Model

The interaction Hamiltonian for the j^{th} ion, given by equation (16), is transformed into the interaction picture with respect to

$$\tilde{H}_c = \sum_{l=1}^{N} (\nu_l - \delta)\, \hat{a}_l^\dagger \hat{a}_l + \frac{\omega_0 - \epsilon}{2} \hat{\sigma}_{z,j} \tag{20}$$

using the unitary operator $\hat{U}_0 = \exp\left[-i\tilde{H}_c t\right]$. The transformed Hamiltonian is is then, according to equation (13):

$$\begin{aligned} \tilde{H}_{I,j} &= \hat{U}_0^\dagger \left(\hat{H}_0 - \tilde{H}_c\right) \hat{U}_0 + \hat{U}_0^\dagger \hat{H}_{I,j} \hat{U}_0 \\ &= \frac{\epsilon}{2} \hat{\sigma}_{z,j} + \delta \hat{a}_l^\dagger \hat{a}_l + \hat{U}_0^\dagger \hat{H}_{I,j} \hat{U}_0 \end{aligned} \tag{21}$$

The interaction term $\hat{U}_0^\dagger \hat{H}_{I,j} \hat{U}_0$ needs to be rewritten, where the outer sum is over the two lasers:

$$\hat{H}_{I,j} = \sum_{n=1}^{2} \Omega_n i \hat{\sigma}_{-,j} e^{i\omega_{j,n} t} e^{i \sum_{l=1}^{N} \eta_{j,n,l} \left(\hat{a}_l + \hat{a}_l^\dagger\right)} + H.C.$$

The two terms are of the same form so only the first will be discussed in the following. The term can be split into an atomic part $\tilde{A}$ and a motional part $\tilde{B}$:

$$\hat{H}_I = \Omega_1 \left\{ \tilde{A} \cdot \tilde{B} + H.C. \right\}$$

where $\hat{A}$ and $\tilde{B}$ are given by:

$$\begin{aligned} \tilde{A} &= e^{i\frac{\omega_0'}{2} t \hat{\sigma_{z,j}}} \hat{\sigma}_{-,j} e^{-i\frac{\omega_0'}{2} t \hat{\sigma_{z,j}}} = \hat{\sigma}_{-,j} - e^{-i\omega_0' t} \\ \tilde{B} &= i e^{i \sum_{l=1}^{N} \nu_l' \hat{a}_l^\dagger \hat{a}_l} e^{-i \sum_{l=1}^{N} \eta_{1,l,j} \left(\hat{a}_l + \hat{a}_l^\dagger\right)} e^{-i \sum_{l=1}^{N} \nu_l' \hat{a}_l^\dagger \hat{a}_l} \approx i + \sum_{l=1}^{N} \eta_{1,l,j} \left(\hat{a}_l e^{-i\nu_l' t} + \hat{a}_l^\dagger e^{i\nu_l' t}\right) \end{aligned}$$

where $\nu_l' = \nu_l - \delta$ and $\omega_0' = \omega_0 - \epsilon$. Both terms were rewritten by using the Baker-Hausdorf lemma:

$$e^{\gamma \hat{O}} \hat{P} e^{-\gamma \hat{O}} = \hat{P} + \gamma \left[\hat{O}, \hat{P}\right] + \frac{\gamma^2}{2!} \left[\hat{O}, \left[\hat{O}, \hat{P}\right]\right] + ...$$

The hermitian conjugate of the first term is $\hat{\sigma}_+ e^{i\omega_0' t}$ and the approximation in the second term is valid in the Lamb-Dicke regime with $\eta \ll 1$, which holds for most ion trap experiments.
Applying the same calculation to the second term yields the following expression, where $n = 1, 2$ denotes whether the term interacts with the first laser field or the second:

$$\begin{aligned} \hat{U}_0^\dagger \hat{H}_{I,j} \hat{U}_0 &\approx \sum_n \Omega_1 e^{i\omega_n t} \hat{\sigma}_{-,j} e^{-i\omega_0' t} \left[i + \sum_{l=1}^{N} \eta_{1,l,j} \left(\hat{a}_l e^{-i\nu_l' t} + \hat{a}_l^\dagger e^{i\nu_l' t}\right) \right] + H.C. \\ &= \sum_n \Omega_1 \hat{\sigma}_{-,j} \left[i e^{i\left(\omega_n - \omega_0'\right) t} + \sum_{l=1}^{N} \eta_{n,l,j} \left(\hat{a}_l e^{-i\left(\nu_l' - \omega_n + \omega_0'\right) t} + \hat{a}_l^\dagger e^{i\left(\nu_l' + \omega_n - \omega_0'\right)}\right) \right] + H.C. \end{aligned}$$

It is advantageous to tune the lasers at the respective side bands: $\omega_1 = \omega_0' - \nu_l'$ and $\omega_2 = \omega_0' + \nu_l'$:

$$\begin{aligned} \hat{U}_0^\dagger \hat{H}_{I,j} \hat{U}_0 \approx\ & \Omega_1 \hat{\sigma}_{-,j} \left[i e^{-i\nu_l' t} + \sum_{l=1}^{N} \eta_{1,l,j} \left(\hat{a}_l e^{i2\nu_l' t} + \hat{a}_l^\dagger\right) \right] \\ & + \Omega_2 \hat{\sigma}_{-,j} \left[i e^{i\nu_l' t} + \sum_{l=1}^{N} \eta_{2,l,j} \left(\hat{a}_l + \hat{a}_l^\dagger e^{i2\nu_l}\right) \right] + H.C. \end{aligned}$$

Only the terms resonant with the side bands contribute significantly to the Hamiltonian, while the other can be neglected in the RWA, yielding:

$$\hat{U}_0^\dagger \hat{H}_{I,j} \hat{U}_0 \approx \Omega_1 \eta_{1,j} \hat{\sigma}_{-,j} \hat{a}^\dagger + \Omega_2 \eta_{2,j} \hat{\sigma}_{-,j} \hat{a} + H.C. \tag{22}$$

This can be rewritten in a simpler form by assuming $\Omega_1 \eta_{1,j} = \Omega_2 \eta_{2,j} \equiv \Omega_p \eta_j$.:

$$\begin{aligned} \hat{U}_0^\dagger \hat{H}_{I,j} \hat{U}_0 &\approx \eta_j \Omega_p \left[\left(\hat{\sigma}_{-,j} \hat{a}^\dagger + \hat{\sigma}_{-,j} \hat{a} \right) + \left(\hat{\sigma}_{+,j} \hat{a} + \hat{\sigma}_{+,j} \hat{a}^\dagger \right) \right] \\ &= \eta_j \Omega_p \hat{\sigma}_{x,j} \left(\hat{a} + \hat{a}^\dagger \right) \end{aligned}$$

Substituting this expression into equation (21) yields the effective interaction Hamiltonian, assuming that $\eta_j = \eta$ for all ions:

$$\hat{H}_I = \sum_{j=1}^{N} \frac{\epsilon}{2} \hat{\sigma}_{z,j} + \delta \hat{a}^\dagger \hat{a} + \eta_j \Omega_p \hat{\sigma}_{x,j} \left(\hat{a} + \hat{a}^\dagger \right) \tag{23}$$

$$= \frac{\epsilon}{2} \hat{J}_z + \delta \hat{a}^\dagger \hat{a} + \eta_j \Omega_p \hat{J}_x \left(\hat{a} + \hat{a}^\dagger \right) \tag{24}$$

which describes the interaction between the two laser fields and the motion of the center-of-mass of the ions.
The parameters can be simplified by introducing the quadrature operator $\hat{x} = \left(\hat{a} + \hat{a}^\dagger \right) / \sqrt{2}$, which corresponds to a dimensionless position operator. The following parameters are also defined: $\lambda = \epsilon/2$ and $\eta'/\sqrt{N} = \eta \Omega_p$, where the factor of $\sqrt{N}$ has been extracted from E_0 from the Rabi frequency $\Omega_p = E_0 D^-$. The quantum number J is taken for the magnitude of the angular momentum to have its maximum value $J = N/2$. Substituting these definitions into equation (23) yields

$$\hat{H} = \lambda \hat{J}_z + \delta \hat{a}^\dagger \hat{a} + \frac{\eta'}{\sqrt{J}} \hat{J}_x \hat{x} \tag{25}$$

The total number of excitations N in the system is the sum of the number of oscillator excitations $\hat{a}^\dagger \hat{a}$, spin excitations J_z and magnitude of the angular momentum j, such that $\hat{N} = \hat{a}^\dagger \hat{a} + \hat{J}_z + j$. The parity operator by can be defined by:

$$\Pi = \exp = \left[i \pi \hat{N} \right] \tag{26}$$

which commutes with the Hamiltonian and thus describes the symmetry of the problem. This operator has the eigenvalues ± 1, depending on whether the number of excitations is even or odd. The Hamiltonian is thus divided in two equivalent subspaces that do not interact with each other, which is the symmetric property of the system.

3.1.1 Phase Transition

We make a mean field description, using the method described in [5], of the Hamiltonian given by equation (25), rewritten in terms of position and momentum operators:

$$\hat{H} = \lambda \hat{J}_z + \frac{\delta}{2} \left(\hat{x}^2 + \hat{p}^2 \right) + \frac{\eta}{\sqrt{J}} \hat{J}_x \hat{x} \tag{27}$$

where the primes have been dropped and the commutator term $[\hat{x}, \hat{p}]$ have been ignored, since they play no role below.
The mean field description to zeroth order is done by assuming that any fluctuations about the different expectation values are negligible, such that $\hat{x}^2 \approx \langle \hat{x} \rangle^2$. The x and z components of the angular momentum are related by:

$$\langle \hat{J}_x \rangle = \sqrt{J^2 - \langle \hat{J}_z \rangle^2} \tag{28}$$

assuming that the system is in the manifold with total angular momentum J. The $\hat{p}^2$ term is also ignored, as it does not contribute to the dynamics. The ground state of the system can be found by minimizing equation (27) in the mean field description:

$$H = \lambda \langle \hat{J}_z \rangle + \frac{\delta}{2} \langle \hat{x} \rangle^2 + \frac{\eta}{\sqrt{J}} \langle \hat{J}_x \rangle \langle \hat{x} \rangle \tag{29}$$

The derivatives are easily found to be:

$$\frac{\partial H}{\partial \langle \hat{x} \rangle} = \delta \langle \hat{x} \rangle + \frac{\eta}{\sqrt{J}} \langle \hat{J}_x \rangle = 0 \tag{30}$$

$$\frac{\partial H}{\partial \langle \hat{J}_z \rangle} = \lambda - \frac{\eta \langle \hat{J}_z \rangle \langle \hat{x} \rangle}{\sqrt{J}\sqrt{J^2 - \langle \hat{J}_z \rangle^2}} = \lambda - \frac{\eta \langle \hat{J}_z \rangle \langle \hat{x} \rangle}{\sqrt{J} \langle \hat{J}_x \rangle} = 0 \tag{31}$$

The first equation can be solved for $\langle \hat{x} \rangle$:

$$\langle \hat{x} \rangle = -\frac{\eta}{\delta\sqrt{J}} \langle \hat{J}_x \rangle \tag{32}$$

which by substitution into the second yields:

$$0 = \lambda + \frac{\eta^2}{J\delta} \langle \hat{J}_z \rangle \tag{33}$$

$$\Rightarrow \langle \hat{J}_z \rangle = -\frac{\lambda\delta}{\eta^2} J \tag{34}$$

This solution only makes sense when $\left|\langle \hat{J}_z \rangle\right| \leq J$, which means that $\eta^2 > \lambda\delta$. We must then have $\langle \hat{J}_z \rangle = -J$ for all values of η^2 less than $\lambda\delta$, which means that there is a sharp transition at $\eta^2 = \lambda\delta \equiv \eta^2_{crit}$ into a state with a non-zero number of excitations of the spin. This phase transmission requirements can be given in terms of the laser properties: $\sqrt{\frac{\epsilon_0 \delta}{2}} = \eta\Omega_p\sqrt{N}$, if the definitions following equation (25) are substituted into $\eta^2 = \lambda\delta$.
Equation (32) shows that there are three regimes for this system: the spin-regime, when $\delta \gg \eta/\sqrt{J}$, where most of the excitations are in the spin. There is a comparable number of excitations in the spin and oscillator in the intermediate regime when $\delta \sim \lambda$ and most excitations in the oscillator when $\lambda \gg \delta$ (the strong-oscillator regime).

3.2 The Boulder Model

This section rewrites the model described in section (2.3.2) with two ions confined in the trap. The first ion is located at $\hat{\bar{r}}_1$ while the second is located at $\hat{\bar{r}}_2$. The position of the i^{th} ion can be written as a deviation $\delta\hat{\bar{r}}_i$ from the equilibrium position $\hat{\bar{r}}_{0,i}$, such that $\hat{\bar{r}}_i = \hat{\bar{r}}_{0,i} + \delta\hat{\bar{r}}_i$. The deviation is the same for the two ions when they are in the COM mode $\delta\hat{\bar{r}}_1 = \delta\hat{\bar{r}}_2 \equiv \delta\hat{\bar{r}}$ and the distance between the ions is: $\hat{\bar{d}} = \hat{\bar{r}}_2 - \hat{\bar{r}}_1 = \hat{\bar{r}}_{0,1} - \hat{\bar{r}}_{0,2}$. The detailed calculations can be found in Appendix (A).
The interaction Hamiltonian is given by the single-ion Hamiltonian plus the contribution from the second ion:

$$\left.\begin{aligned} \hat{H}_I = &|0\rangle\langle e| \left(e^{i\bar{k}_1\hat{\bar{r}}_1}\alpha_{10}e^{-i\omega_1 t} + e^{i\bar{k}_2\hat{\bar{r}}_1}\alpha_{20}e^{-i\omega_2 t} + e^{i\bar{k}_1\hat{\bar{r}}_2}\alpha_{10}e^{-i\omega_1 t} + e^{i\bar{k}_2\hat{\bar{r}}_2}\alpha_{20}e^{-i\omega_2 t}\right) + H.C. \\ &+ |1\rangle\langle e| \left(e^{i\bar{k}_1\hat{\bar{r}}_1}\alpha_{11}e^{-i\omega_3 t} + e^{i\bar{k}_2\hat{\bar{r}}_1}\alpha_{21}e^{-i\omega_4 t} + e^{i\bar{k}_1\hat{\bar{r}}_2}\alpha_{11}e^{-i\omega_3 t} + e^{i\bar{k}_2\hat{\bar{r}}_2}\alpha_{21}e^{-i\omega_4 t}\right) + H.C. + \Delta|e\rangle\langle e| \end{aligned}\right\} \tag{35}$$

where the laser phases have been absorbed into the states: $|0\rangle = e^{i\phi}|\tilde{0}\rangle$ and $|1\rangle = e^{i\phi}|\tilde{1}\rangle$. The total phase $\Phi_i = \phi + \hat{\bar{r}}_{i,0}$ is not absorbed, because of interference effects due to the position of the ions. This will be explained in detail later in this section.

We consider an arbitrary state $|\psi\rangle = c_0|0\rangle + c_1|1\rangle + c_e|e\rangle$, which, by plugging into the Schrödinger equation $i\frac{\partial|\psi\rangle}{\partial t} = \hat{H}_I|\psi\rangle$, gives a set of coupled differential equations for the coefficients. The coefficient for the third energy level is adiabatically eliminated by setting $\dot{c}_e = 0$, by assuming that all ions start out in the ground state, and that the interaction quickly deexcites the third level, leaving it essentially unpopulated for the duration of the experiment. This yields:

$$c_e = -\frac{1}{\Delta}\left\{\begin{array}{c} c_0\left(e^{-i\overline{k}_1\hat{\overline{r}}_1}\alpha_{10}e^{i\omega_1 t} + e^{-i\overline{k}_2\hat{\overline{r}}_1}\alpha_{20}e^{i\omega_2 t} + e^{-i\overline{k}_1\hat{\overline{r}}_2}\alpha_{10}e^{i\omega_1 t} + e^{-i\overline{k}_2\hat{\overline{r}}_2}\alpha_{20}e^{i\omega_2 t}\right) \\ +c_1\left(e^{-i\overline{k}_1\hat{\overline{r}}_1}\alpha_{11}e^{i\omega_3 t} + e^{-i\overline{k}_2\hat{\overline{r}}_1}\alpha_{21}e^{i\omega_4 t} + e^{-i\overline{k}_1\hat{\overline{r}}_2}\alpha_{11}e^{i\omega_3 t} + e^{-i\overline{k}_2\hat{\overline{r}}_2}\alpha_{21}e^{i\omega_4 t}\right)\end{array}\right\} \tag{36}$$

which, by inserting into the equations for $\dot{c}_0$ and $\dot{c}_1$, yields a set of differential equations for the remaining coefficients. The lasers are tuned at:

$$\begin{array}{cc} \omega_1 - \omega_2 = \delta - \nu = \omega_3 - \omega_4 & \omega_3 - \omega_1 = -\omega_0 = \omega_4 - \omega_2 \\ \omega_3 - \omega_2 = \delta - \omega_0 - \nu & \omega_4 - \omega_1 = \nu - \omega_0 - \delta \end{array}$$

This choice of laser frequencies causes the terms containing $\alpha_{ij}^2, \alpha_{20}\alpha_{11}$ and $\alpha_{10}\alpha_{21}$ to be approximately zero.
It is known from atomic physics that $\alpha_{10}\alpha_{20} = -\alpha_{11}\alpha_{21}$ and $\alpha_{20}\alpha_{11} = \alpha_{10}\alpha_{21}$. The two lasers are directed at right angles and we have, assuming that $\overline{k}_i \parallel \hat{\overline{r}}_i$, from which it follows that $\overline{k}_2 \perp \hat{\overline{r}}_1$ and $\overline{k}_1 \perp \hat{\overline{r}}_2$. It is also assumed that $\overline{k}_1 \perp \hat{\overline{r}}_1 \approx \overline{k}_2 \perp \hat{\overline{r}}_2$. It can be shown the interaction Hamiltonian reduces to:

$$\hat{H}_I = \left\{\begin{array}{l} \frac{\alpha'_{10}\alpha'_{20}E_0^2 D^- D^+}{2\Delta}\hat{\sigma}_z\left[e^{i(\nu-\delta)t}\left(e^{-i\Delta\overline{k}\hat{\overline{r}}_1} + e^{-i\Delta\overline{k}\hat{\overline{r}}_2}\right) + e^{-i(\nu-\delta)t}\left(e^{i\Delta\overline{k}\hat{\overline{r}}_1} + e^{i\Delta\overline{k}\hat{\overline{r}}_2}\right)\right] \\ +\left(\frac{\alpha'_{10}\alpha'_{11}E_0^2 D^- D^+}{4\Delta}\hat{\sigma}_+ e^{-i\omega_0 t}\left[e^{i\overline{k}_1\hat{\overline{d}}} + e^{-i\overline{k}_1\hat{\overline{d}}} + e^{i\overline{k}_2\hat{\overline{d}}} + e^{-i\overline{k}_2\hat{\overline{d}}}\right] + H.C.\right)\end{array}\right\} \tag{37}$$

where the expressions for α_{ij} have been inserted. The Rabi frequencies are defined as

$$\Omega_p \equiv \frac{\alpha'_{10}\alpha'_{20}E_0^2 D^- D^+}{2\Delta} \tag{38}$$

$$\Omega_x \equiv \frac{\alpha'_{10}\alpha'_{11}E_0^2 D^- D^+}{\Delta} \tag{39}$$

The spatial exponentials need to be rewritten. For the first term in equation (37):

$$\begin{aligned} e^{i\Delta\overline{k}\delta\hat{\overline{r}}}\left[e^{i\Delta\overline{k}\hat{\overline{r}}_{0,1}} + e^{i\Delta\overline{k}\hat{\overline{r}}_{0,2}}\right] &= e^{i\Delta\overline{k}\delta\hat{\overline{r}}}e^{i\Delta\overline{k}\frac{\hat{\overline{r}}_{0,1}+\hat{\overline{r}}_{0,2}}{2}}\left(e^{i\Delta\overline{k}\frac{\hat{\overline{r}}_{0,1}-\hat{\overline{r}}_{0,2}}{2}} + e^{-i\Delta\overline{k}\frac{\hat{\overline{r}}_{0,1}-\hat{\overline{r}}_{0,2}}{2}}\right) \\ &= 2e^{i\Delta\overline{k}\delta\hat{\overline{r}}}e^{i\Delta\overline{k}\frac{\hat{\overline{r}}_{0,1}+\hat{\overline{r}}_{0,2}}{2}}\cos\left(\Delta\overline{k}\frac{\hat{\overline{r}}_{0,1} - \hat{\overline{r}}_{0,2}}{2}\right) \\ &= 2e^{i\Delta\overline{k}\delta\hat{\overline{r}}}e^{i\Delta\overline{k}\frac{\hat{\overline{r}}_{0,1}+\hat{\overline{r}}_{0,2}}{2}}\cos\left(\frac{\Delta\overline{k}\ \hat{\overline{d}}}{2}\right) \end{aligned} \tag{40}$$

The cosine-part shows that constructive interference occurs when

$$\overline{k}\ \hat{\overline{d}} = 2\pi p, \quad p \in \mathbb{Z} \tag{41}$$

which also ensures that $e^{i\Delta\overline{k}\frac{\hat{\overline{r}}_{0,1}+\hat{\overline{r}}_{0,2}}{2}} = 1$ due to the periodicity of the interference pattern. For the second term in equation (37)

$$e^{\pm i\overline{k}_1\hat{\overline{d}}} + e^{\pm i\overline{k}_2\hat{\overline{d}}} = 2e^{\pm\frac{i\hat{\overline{d}}(\overline{k}_1+\overline{k}_2)}{2}}\cos\left(\frac{\overline{k}\ \hat{\overline{d}}}{2}\right) \tag{42}$$

where this term have the same requirement for constructive interference, $\Delta\overline{k}\ \hat{\overline{d}} = 2\pi p$. Inserting equations (40) and (42) into equation (37) gives:

$$\hat{H}_I = \Omega_p\hat{\sigma}_z\left[e^{i(\nu-\delta)t}e^{-i\Delta\overline{k}\delta\hat{\overline{r}}} + e^{-i(\delta-\nu)t}e^{i\Delta\overline{k}\delta\hat{\overline{r}}}\right] + \left(\Omega_x e^{i\Delta\overline{k}\delta\hat{\overline{r}}}\hat{\sigma}_+ e^{-i\omega_0 t} + H.C.\right) \tag{43}$$

The change to the interaction picture is done with respect to

$$\hat{H}_c = (\nu - \delta)\,\hat{a}^\dagger\hat{a} + \frac{\omega_0}{2}\hat{J}_z \tag{44}$$

The procedure is the same as in section (3.1) by using standard quantum optics methods. The two-ion interaction Hamiltonian in the RWA is then:

$$\hat{H}_I = \delta\hat{a}^\dagger\hat{a} + \frac{\Omega_x}{2}\hat{J}_x + \eta\Omega_p\hat{J}_z i\left(\hat{a} - \hat{a}^\dagger\right) \tag{45}$$

The ions need to be located in this constructive interference zone, as defined by the cosine part in equation (41), to maximize the atomic response to the laser fields. This is relatively simple to realize for two ions but it becomes progressively harder for higher number of ions as the distance between the i^{th} and j^{th} ions will in general differ from the distance between the k^{th} and l^{th} ions due to the Coulomb force between the ions. The combination of the Coulomb force and the more complicated electric field in the Boulder model makes this model somewhat harder to realize. The Innsbruck model may be preferable if the aim for an experiment is to examine the behaviour of phase transition for high ion numbers.

3.2.1 Phase Transition

The mean field description of the Hamiltonian given by equation (45) is done using the same procedure as in section (3.1.1). The derivatives are taken with respect to $\langle\hat{p}\rangle$ and $\langle\hat{J}_x\rangle$ instead, which yields

$$\langle\hat{x}\rangle = -\frac{\eta}{\delta\sqrt{J}}\langle\hat{J}_z\rangle$$
$$\langle\hat{J}_x\rangle = -J\frac{\lambda\delta}{\eta^2}$$

which has the same requirements for the phase transition as in the Innsbruck model. The processes are essentially the same: all ions in the Innsbruck model are prepared in the spin-z configuration but abruptly change to the spin$-x$ configuration as the Lamb-Dicke parameter η increases. The ions in the Boulder model undergoes the same transition, but in the opposite direction: from the spin$-x$ configuration to the spin$-z$ configuration. Only consider the Hamiltonian for the Innsbruck model will be considered in the following, as the two Hamiltonians essentially describe the same dynamics.

3.3 Description Through Holstein-Primakoff Transformations

This section follows the procedure presented in reference [3] and the detailed calculations can be found in Appendix (B). The phase transition is best explained by rewriting the Hamiltonian, given by equation (25), using the Holstein-Primakoff transformations by expressing the atomic angular momentum operators in terms of creation $\hat{b}$ and annihilation $\hat{b}^\dagger$ operators of a second mode of light:

$$\hat{J}_+ = \hat{b}^\dagger\sqrt{2J - \hat{b}^\dagger\hat{b}} \tag{46}$$

$$\hat{J}_- = \sqrt{2J - \hat{b}^\dagger\hat{b}}\hat{b} \tag{47}$$

$$\hat{J}_z = \hat{b}^\dagger\hat{b} - J \tag{48}$$

The Hamiltonian from equation (25) is in this representation:

$$\hat{H} = \lambda\left(\hat{b}^\dagger\hat{b} - j\right) + \delta\hat{a}^\dagger\hat{a} + \eta'\left(\hat{a} + \hat{a}^\dagger\right)\left(\hat{b}^\dagger\sqrt{1 - \frac{\hat{b}^\dagger\hat{b}}{2J}} + \sqrt{1 - \frac{\hat{b}^\dagger\hat{b}}{2J}}\hat{b}\right) \tag{49}$$

where $\lambda = \epsilon/2$ and $\eta' = \eta/2$. The parity operator, given by equation (26), is:

$$\Pi = \exp\left[i\pi\left(\hat{a}^\dagger\hat{a} + \hat{b}^\dagger\hat{b}\right)\right] \tag{50}$$

The the lack of both population inversion and oscillator excitations in this normal phase can be explained by the spatial distribution of the atoms. Light will scatter of the atoms and will in general destructively interfere with light scattered from nearby ions, no cavity field will then build up, i.e. $\hat{a}^\dagger\hat{a} = 0$ and there will not be any excitations. The ions will tend to position themselves according to the constructive interference pattern defined by equation (41), strengthening the response of the atoms.

3.3.1 The Normal Phase

A mean field description equivalent to that in section (3.1.1) can be made by neglecting terms with J in the denominator in equation (49), assuming that we take the thermodynamical limit $N \to \infty$, which yields a Hamiltonian of the form:

$$\hat{H} = \lambda \hat{b}^\dagger \hat{b} + \delta \hat{a}^\dagger \hat{a} + \eta' \left(\hat{a} + \hat{a}^\dagger\right)\left(\hat{b} + \hat{b}^\dagger\right) - J\lambda \tag{51}$$

This Hamiltonian can be diagonalized by introducing position, $\hat{x}$ and $\hat{y}$, and momentum $\hat{p}_x$ and $\hat{p}_y$ operators for the two bosonic fields. The diagonalized Hamiltonian is:

$$\hat{H} = \frac{1}{2}\left[\epsilon_-^2 q_1^2 + p_1^2 + \epsilon_+^2 q_2^2 + p_2^2 - \delta - \lambda\right] - J\lambda \tag{52}$$

which has the form of two uncoupled harmonic oscillators, where

$$\epsilon_\pm^2 = \frac{1}{2}\left[\delta^2 + \lambda^2 \pm \sqrt{(\delta^2 - \lambda^2) + 16\eta'^2\lambda\delta}\right] \tag{53}$$

The energies need to be real, so we need to set;

$$\delta^2 + \lambda^2 > \sqrt{\left(\lambda^2 - \delta^2\right)^2 + 16\eta'^2\lambda\delta} \Rightarrow \eta' < \frac{\sqrt{\lambda\delta}}{2} \Rightarrow \eta < \sqrt{\lambda\delta} \tag{54}$$

which is the same phase transition condition as in section (3). Note that the parity operator given by equation (50) still commutes with the Hamiltonian, so the symmetry of the system is still preserved.

3.3.2 The Excited Phase

A mean field description to first order can be made by modifying the bosonic modes to have macroscopic displacements, corresponding to the macroscopic excitations shown in section (4.1):

$$\hat{a} \to \hat{c} \pm \sqrt{\alpha}, \quad \hat{b} \to \hat{d} \mp \sqrt{\beta} \tag{55}$$

where the choice of sign is arbitrary, except for a few changes of sign in the following. The final result is the same regardless of the choice of sign. The Hamiltonian becomes:

$$\left.\begin{aligned}\hat{H} =& \lambda\left[\hat{d}^\dagger\hat{d} - \sqrt{\beta}\left(\hat{d} + \hat{d}\right) + \beta - j\right] + \delta\left[\hat{c}^\dagger\hat{c} + \sqrt{\alpha}\left(\hat{c} + \hat{c}^\dagger\right) + \alpha\right] \\ &+ \eta'\sqrt{\frac{2j-\beta}{2j}}\left[\hat{c} + \hat{c}^\dagger + 2\sqrt{\alpha}\right]\left[\hat{d}^\dagger K + K\hat{d} - 2\sqrt{\beta}K\right]\end{aligned}\right\} \tag{56}$$

where

$$K = \sqrt{1 - \frac{\hat{d}^\dagger\hat{d} - \sqrt{\beta}\left(\hat{d} + \hat{d}^\dagger\right)}{2j - \beta}} \simeq 1 - \frac{\hat{d}^\dagger\hat{d} - \sqrt{\beta}\left(\hat{d} + \hat{d}^\dagger\right)}{2\left(2j - \beta\right)}$$

The first-order mean field description is done by expanding K to first order and eliminate terms linear in $\hat{c}$ and $\hat{d}$ by choosing

$$\sqrt{\alpha} = \frac{2\eta'}{\delta}\sqrt{\frac{j}{2}\left(1 - \mu^2\right)} \tag{57}$$

$$\sqrt{\beta} = \sqrt{j\left(1 - \mu\right)} \tag{58}$$

where $\mu = \frac{\delta\lambda}{4\eta^2}$. The Hamiltonian can be simplified by introducing position and momentum operators similarly to the previous section. The resulting Hamiltonian is:

$$\hat{H}_1 = \epsilon_-^{(1)}\hat{e}_1^\dagger\hat{e}_1 + \epsilon_+^{(1)}\hat{e}_2^\dagger\hat{e}_2 - j\left[\frac{2\eta'^2}{\delta} + \frac{\lambda^2\delta}{8\eta'^2}\right] + \frac{1}{2}\left[\epsilon_+^{(1)} + \epsilon_-^{(1)} - \frac{\delta}{2\mu}\left(1 + \mu\right) - \lambda - \frac{2\eta'^2}{\lambda}\left(1 - \mu\right)\right] \tag{59}$$

The oscillator energies are given by:

$$2\epsilon_{\pm}^{(1)} = \frac{\lambda^2}{\mu^2} + \delta^2 \pm \sqrt{\left[\frac{\lambda^2}{\mu^2} - \delta^2\right]^2 + 4\lambda^2\delta^2} \tag{60}$$

These energies also need to be real, which gives that $\eta > \delta\lambda$, so this Hamiltonian hold for values of η above the phase transition. These energies do not depend on the choice of sign in equation (55), so the states are degenerate. It can be shown that this Hamiltonian does not commute with the parity operator from equation (26), thus breaking the global symmetry of the system. But two local symmetries appear, corresponding to a new parity operator:

$$\Pi_1 = \exp\left[i\pi\left(\hat{c}^\dagger\hat{c} + \hat{d}^\dagger\hat{d}\right)\right] \tag{61}$$

for either choice of displacement. This kind of symmetry-break indicates that the system can be described by the double-well potential, which has the general form: $V(x) = \alpha x^2 + \beta x^4$. Each atom in the ensemble will in the normal phase be found in the bottom of the a harmonic oscillator potential but will spontaneously jump to one of the new potential wells as the symmetry is broken. The atoms will be randomly distributed between the two wells and the population in one of the wells will in general differ slightly from the other. The destructive interference effects described at the start of this section will no longer hold and a cavity field will begin to build up, i.e. $\hat{a}^\dagger\hat{a} \neq 0$, so the light will excite some of the ions. The electric fields in both the Innsbruck model and the Boulder model have the forms $E_1 = E_0\cos(k_1 r_{1,0})$ and $E_2 = E_0\cos(k_2 r_{2,0})$, where the small deviation δr_i from the equilibrium position have been excluded to simplify the following equation. The potential associated with these fields is:

$$V(r_{1,0}, r_{2,0}) = E_0^2\cos^2(k_1 r_{1,0}) + E_0^2\cos^2(k_2 r_{2,0}) \pm 2E_0^2\cos(k_1 r_{1,0})\cos(k_2 r_{2,0}) \tag{62}$$

where the sign of the last term depend on the phases of the lasers. The last term corresponds to the constructive interference condition of equation (41) and will increase one of the wells in the potential. This increased minima will attract more ions, which will further increase the effective strength of the cavity field, giving more excitations. This results in a runaway process, which gives rise to the sudden population inversion. This is shown in figure (3) in section (4.1).
Both of these results are derived in the thermodynamical limit, where $N \to \infty$. It is then expected that the phase transition behaves similarly for any number of ions, as long as $N \gg \langle\hat{b}^\dagger\hat{b}\rangle$. This is examined in section (4.3).

4 Numerical Analysis

4.1 The Ground State

It has been shown in sections (3.1.1) and (3.2.1) that the expectation value for the $z-$component of the spin $\langle\hat{J}_z\rangle$ has a phase transition to the lowest possible value $\langle\hat{J}_z\rangle = -J$ when $\eta^2 = \delta\lambda$. Further insight into the behaviour of the phase transition can be gained from a direct diagonalization of the Hamiltonian for the Innsbruck model for various values of the ratio λ/δ, given by (25). Only the Hamiltonian for the Innsbruck model is considered, since this Hamiltonian and the Hamiltonian for the Boulder model are equivalent. The Hamiltonian can be made dimensionless by dividing with a characteristic frequency. A suitable choice is the critical value of the Lamb-Dicke parameter, $\eta_{crit} = \sqrt{\delta\lambda}$, such that the rescaled Hamiltonian is:

$$\frac{\langle\hat{H}\rangle}{\sqrt{\delta\lambda}} = \sqrt{\frac{\lambda}{\delta}}\langle\hat{J}_z\rangle + \frac{1}{2}\sqrt{\frac{\delta}{\lambda}}\langle\hat{a}^\dagger\hat{a}\rangle + \frac{\eta}{\sqrt{\delta\lambda}J}\langle\hat{J}_x\rangle\langle\hat{x}\rangle \tag{63}$$

This ensures that the phase transition will happen at $\eta \approx 1$ for any value of λ/δ. These value are chosen such that each of the three regimes described in section (3.1.1) The expectation value of $\hat{J}_z$ is computed for a varying value of η for each λ/δ. The results are plotted in figure (3). A reference to the Matlab script for the diagonalization, and for the subsequent numerical treatments, can be found in section (6.1).

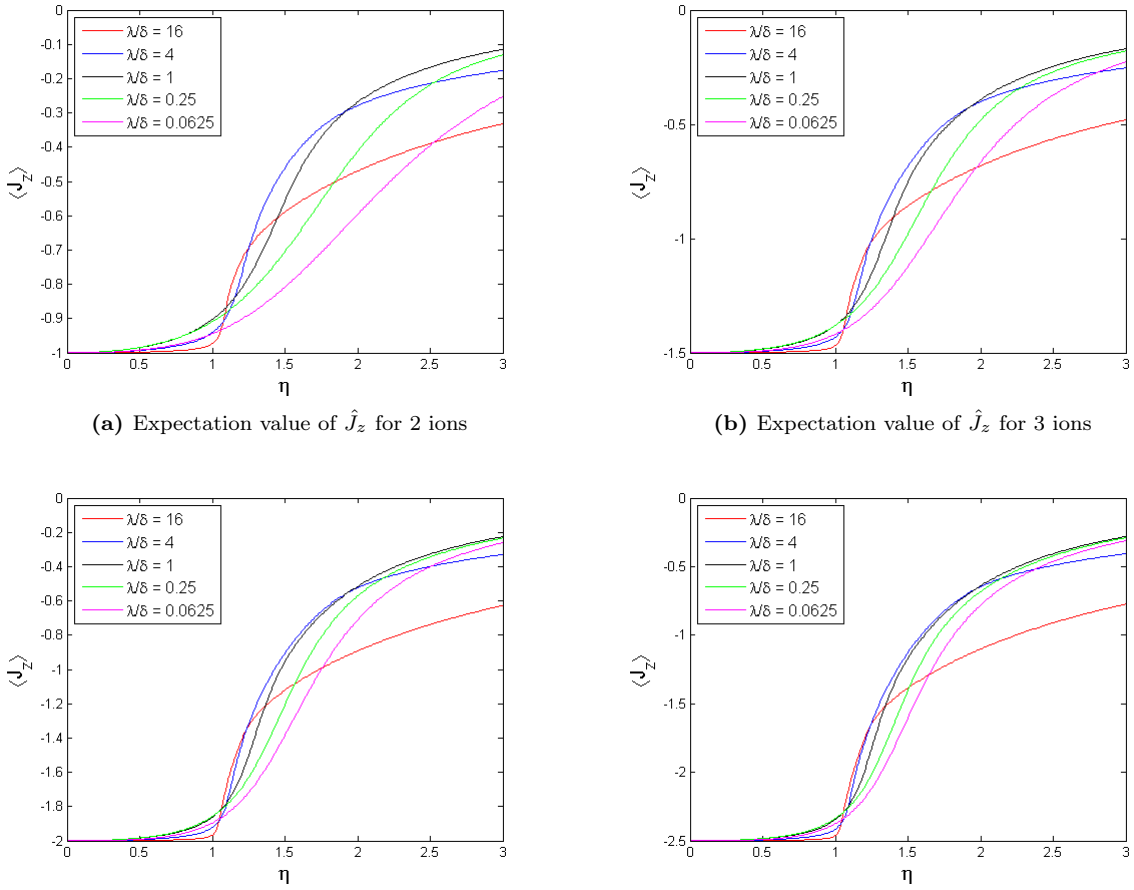

(a) Expectation value of $\hat{J}_z$ for 2 ions

(b) Expectation value of $\hat{J}_z$ for 3 ions

(c) Expectation value of $\hat{J}_z$ for 4 ions

(d) Expectation value of $\hat{J}_z$ for 5 ions

Figure 3: Plots of phase transitions for various number of ions and ratios λ/δ for the Innsbruck model

The diagonalization reveals that the transition gets sharper for high values of λ/δ across all values of N and that the phase transition is essentially non-existent in the intermediate- and the spin regimes, regardless of the number of ions. This seems to suggest that the system needs to be prepared in the strong-oscillator regime to permit the phase transition. The expectation value of the number of oscillator excitations $\hat{n} = \hat{a}^\dagger \hat{a}$ has been found in the same manner for $N = 5$. The plots are presented in figure (4) The expectation value of the number of excitations in the oscillator follows the same pattern: The number of excitations suddenly rises at $\eta^2 = \lambda\delta$ when $\lambda > \delta$, while the increase in excitations are a lot slower in the spin regime $\lambda < \delta$. This conforms with the equation (32) in section (3). A plot for the Boulder model is shown in Appendix (D.3) It is clearly seen that the two models undergo the same phase transition at $\eta = \eta_{crit} = \lambda\delta$.
The diagonalization also seems to indicate that the number of ions is not important for the phase transition, as it behaves in the same way for all the examined values of N. This behaviour will be examined more thoroughly in section (4.3).

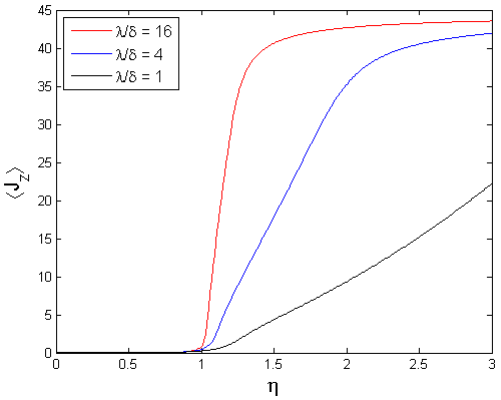

(a) Expectation value for $\langle \hat{a}^\dagger \hat{a} \rangle$ with $\lambda/\delta = 16, 4, 1$

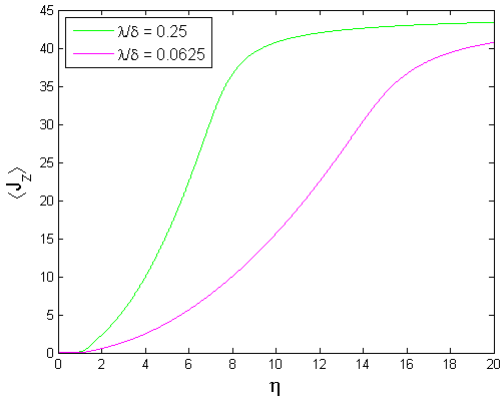

(b) Expectation value for $\langle \hat{a}^\dagger \hat{a} \rangle$ with $\lambda/\delta = 1/4, 1/16$

Figure 4: Expectation value for $\hat{n} = \hat{a}^\dagger \hat{a}$ for $N = 5$. Note the high values for plot (b)

4.2 Adiabatic Parameters

The existence of the phase transition has been demonstrated in sections (3.1.1) and (3.3) by examining the ground state in the former section, and by examining the dependence on η in the latter. This section continues the examination of η by numerically testing various time-dependent linear models for η. This section also demonstrates the need to evolve $\eta(t)$ adiabatically slow to be able to measure the phase transition and to be able to do so with minimal error.
The conditions for the adiabatic increase in $\eta(t)$ for the system is examined by numerically solving the time-dependent Schrödinger equation $i\frac{\mathrm{d}|\psi\rangle}{\mathrm{d}t} = \hat{H}|\psi\rangle$ for various linear models for $\eta(t)$ using the ODE45 solver in Matlab. The Matlab scripts are described in section (6.1).

4.2.1 Linear Lamb-Dicke Parameter $\eta(t)$

The Schrödinger equation has been numerically solved for four different models for a linear increase in $\eta(t) \propto kt$, where $k = 10^{-3}, 10^{-2}, 10^{-1}$, going from a slow, adiabatic increase in $\eta(t)$ to a rapid increase. The solution is plotted against the results from the diagonalization of the ground state to examine the effect on the phase transition. This is done for a system containing three ions in the strong oscillator regime $\lambda/\delta = 16$, where the phase transition is prominent. The deviation from the ground state, ϵ, have been defined as:

$$\epsilon = \left| \langle \hat{J}_z \rangle_{Time} - \langle \hat{J}_z \rangle_{Ground} \right| \tag{64}$$

where $\langle \hat{J}_z \rangle_{Time}$ is the expectation value of $\hat{J}_z$ from the solution to the Schrödinger equation and $\langle \hat{J}_z \rangle_{Ground}$ is the expectation value from the ground state. The results for the expectation values and the errors are plotted against $\eta(t)$ in figure (5).
Plot (a) and (b) in figure (5) show that a fast increase in $\eta(t)$, corresponding to $k = 0.01$ and $k = 0.1$, do not follow the ground state. It is also seen that the deviation with respect to the ground state is large at the phase transition and remains significant for high values of $\eta(t)$. The models for $\eta(t)$ will therefore not permit a measurement of the phase transition. The slow model, with $\eta(t) = 10^{-3}t$, closely follows the ground state with little deviation. This indicates that a slope of 10^{-3} is of the right order of magnitude to permit a measurement of the phase transition. A fast increase in $\eta(t)$ drives the population inversion faster than the change in the electric field, preventing the field to split the potential into the double-well potential and thereby the spontaneous symmetry breaking described in section (3.3) will not take place. Plot (c) and (d) in figure (5) shows the same situation for slowly evolving $\eta(t)$ ranging between $k = 10^{-3}$ and $k = 10^{-2}$. It is seen that these cases rapidly approach the ground state, as the slope of $\eta(t)$ is lowered, giving the electric field time to split into the double-well potential.
The very slow models with $k = 10^{-3}$ and $2 \cdot 10^{-3}$ in particular stand out, with negligible deviation

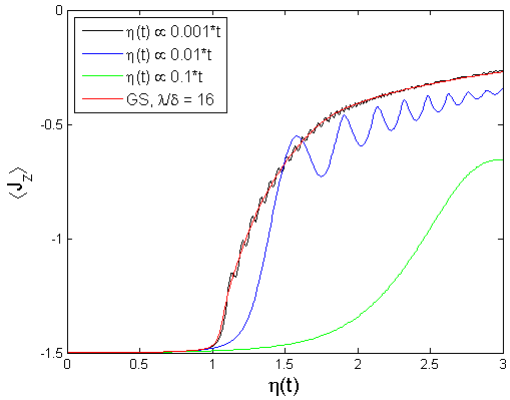

(a) Population inversion for $N = 3$ for various $\eta(t)$models

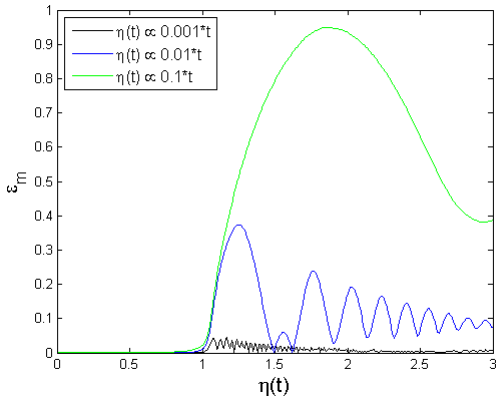

(b) The deviation from the ground state for the models

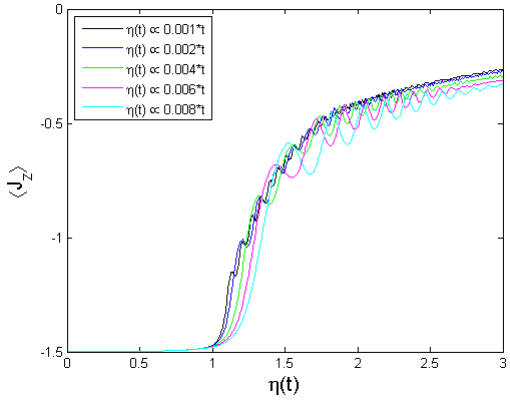

(c) Population inversion for $N = 3$ for various $\eta(t)$models

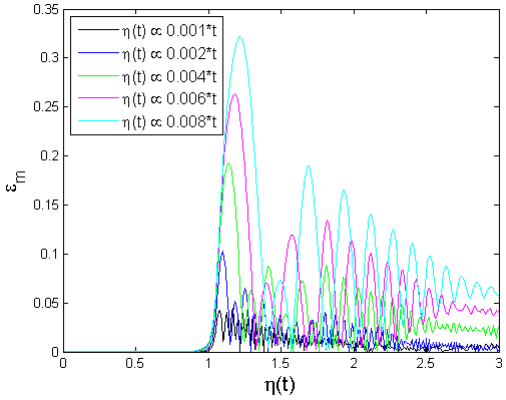

(d) The deviation from the ground state for the models

Figure 5: Population inversion and error for $N = 3, \lambda/\delta = 16$ for various $\eta(t)$-models

from the ground state. Both of these models should permit a measurement of the phase transition; it is possible that the remaining of the slow models also permit this measurement, but the possibility to do so rapidly decreases. Appendix (D.1) shows additional plots for $N = 2, 4, 5$ to test the behaviour with a different number of ions trapped. It is seen that the number of ions do not change the behaviour of the phase transition significantly, as was seen in section (4.1). This is further discussed in section (4.3).

A similar plot is shown in figure (6) but shows the mean deviation ϵ_m from the ground state against the different slopes $\frac{\mathrm{d}\eta}{\mathrm{d}t}$ and for various values of λ/δ, ranging from $\lambda/\delta = 4$ to $\lambda/\delta = 20$, i.e. from the intermediate regime to the strong-oscillator regime. The intermediate regime is included for reference, while the strong-spin regime is excluded since this regime does not allow the phase transition, as was described in the previous section. Figure (6) further shows the importance of driving the system adiabatically slow in the strong-oscillator regime, as it is seen that the deviation rapidly rises in this case. Note that this difference in the deviation is almost negligible in the intermediate regime. Additional plots are shown in Appendix (D.2) for $N = 2, 4, 5$ shows that the deviation behaves in the same manner for the different cases, but that the mean deviations rise slightly with the number of ions.
This section then provides the information about the parameters λ, δ and $\eta(t)$, that is necessary to experimentally measure the phase transition, provided that $\eta(t)$ increases linearly in time and that the value of λ and δ is fixed in the strong-oscillator regime, $\lambda \gg \delta$. $\eta(t)$ needs to be driven adiabatically, preferably around $\eta(t) \propto 10^{-3}t$. Figures (5) and (6) suggests that a reasonable upper bound for the deviation is about $\epsilon_m = 0.1$, as the slowest models described in figure (5,c) fulfils this.

4.3 Universality of the Phase Transition

The universality of the phase transition is examined by examining the relationship between the optimal slopes and the second derivative of $\langle \hat{J}_z \rangle$ for various values of λ/δ and N. The second derivative is used, as the phase transition is of second order [3] and we work with scaled parameters $\langle \hat{J}_z \rangle / N$ and $\epsilon_m = \left| \langle \hat{J}_z \rangle_{Time} - \langle \hat{J}_z \rangle_{GS} \right| / N$ to test the universality. The upper bound of the deviation is set to $\epsilon_m / N = 0.015$, which correspond to $\epsilon_m \approx 0.1$ for each N. The Schrödinger equation is then solved and $\frac{\mathrm{d}\eta(t)}{\mathrm{d}t}$ corresponding the chosen upper bound is found. This slope is plotted against the second derivative evaluated at the phase transition in figure (7) for $N = \{2, 5\}$ to test for a varying number of ions of ions and for $\lambda/\delta = \{8, 20\}$ to test both the intermediate region and in the strong-oscillator regime.
Figure (7) shows that the systems behave in the same manner at the phase transition, with small differences due to the resolution of the program. This provides evidence of the universality of the system. It should thus be possible to measure the phase transition for any number of ions, provided that η is driven adiabatically slow.

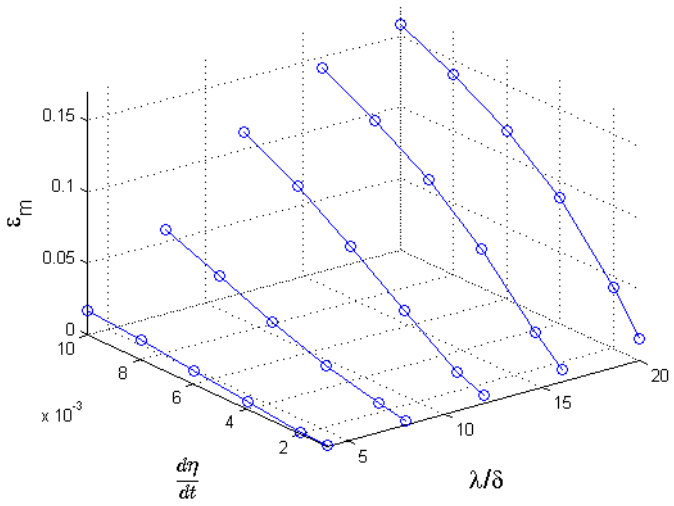

Figure 6: The mean deviation ϵ_m from the ground state for various λ/δ and $\mathrm{d}\eta/\mathrm{d}t$

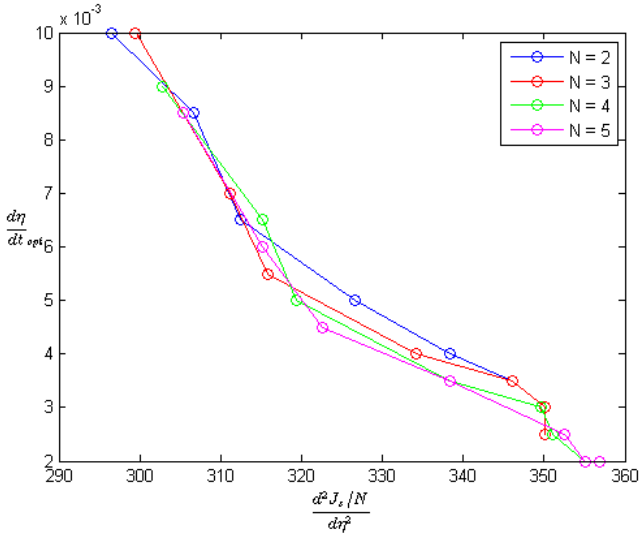

Figure 7: Test of the universality of the phase transition for various numbers N of ions and ratios λ/δ

5 Conclusion and Outlook

5.1 Conclusion

This thesis has demonstrated the existence of a phase transition in the expectation value of $\langle \hat{J}_z \rangle$ in the Dicke model, realized in the models used by the research groups in Innsbruck and Boulder. It has also been shown that the phase transition is strongest in the regime where there are lot of excitations in the oscillations of the ions in the trap.
The importance of driving the Lamb-Dicke parameter $\eta(t)$ adiabatically slow has been demonstrated; this reduces the deviations from the expectation value for the ground state, provided that $\eta(t)$ is driven linearly in time, with the optimal model $\eta(t) \approx 10^{-3}t$. It has been shown how the phase transition breaks down if either the system is not prepared in the strong-oscillator regime or if the Lamb-Dicke parameter is driven too fast. It should be possible to measure the phase transition for any number of ions, as the universality of the phase transition has also been shown to hold.

5.2 Outlook

The analysis in section (4.2) is limited, due to the fact that only η evolves in time, while λ and δ stay at fixed values. Further insight can be gained by letting λ or δ (or both) evolve in time. The significance of the model used for $\eta(t)$ can also be further examined by inputting different models into the Matlab script. More realistic models can also be considered, for example a model where $\eta(t)$ is only adiabatically driven close to the phase transition point $\eta = \sqrt{\lambda/\delta}$ and fast otherwise can be used, which may be easier to implement in a experimental set up.

The properties of the phase transition can also be studied in further detail, with emphasis on the order parameter, i.e. the first derivative of the energy, and the dependence of the adiabatic evolution of $\eta(t)$. The corresponding classical system, i.e. the coupling between two harmonic oscillators, shows chaotic properties at the phase transition [3], and there is a possibility that the Dicke model can be used to make a proper description of quantum chaos.

6 References

1. J. Benhelm, G. Kirchmair, C. F. Roos, R. Blatt, *Towards fault-tolerant quantum computing with trapped ions*, Nature Physics **4**, 463 (2008)

2. D. Liebfied *et al*, *Experimental demonstration of a robust, high-fidelity geometric two ion-qubit phase gate*, Nature Physics **422**, 412-415 (2003)

3. T. Brandes, C. Emary, *Chaos and the quantum phase transition in the Dicke model*, Physical Review E **67**, 066203 (2003)

4. C. C. Gerry, P. L. Knight, *Introductory Quantum Mechanics* (Cambridge University Press, Cambridge, ed. 1, 2005), pp. 10-15

5. A. S. Sørensen, *Quantum Phase Transition in an Ion Trap*, Theoretical Quantum Optics Group, Niels Bohr Institute, Note

6.1 Matlab Programs

The program Matlab R2013a developed by Mathworks have been used in the numerical treatment for this thesis. The main m-files are ordered in to three sub-folders, depending on the problem. Most of the files are identical but are used differently for each problem. TimePhase_vOne is used to plot $\langle \hat{J}_z \rangle$ against $\eta(t)$ for various models of $\eta(t)$ and TimePhase_vTwo is used to plot the error for various models of $\eta(t)$ and ratios of λ/δ. The results for these scripts are presented in section (4.2). TimePhase_vThree tests the universality, as described in section (4.3).
These folders are posted on the internet at (https://www.dropbox.com/s/hjaolxgl0n1g0yo/MatlabScripts.zip) and is not presented here, as the length of the code is considerable.

Shared m-files

- **Parameters.m**: This m-file defines the various parameters used.
- **Phase.m**: This program defines the various matrices used by the rest of the programs
- **HFunc.m**: This function defines the time-dependant Hamiltonian as a function. The time-dependance is only entered through the function eta.m
- **Deriv.m**: This function defines the time-dependant Schrödinger equation as $|\dot{\psi}\rangle = -i\hat{H}\,|\psi\rangle$
- **TimeSolve.m**: This program solves the time-dependant Schrödinger equation and saves the results in convenient vectors
- **eta.m**: This function defines eta as a time-dependant function. Note the functions lambda.m and delta.m - these are set equal to one in this thesis, but can easily be changed to a time-dependant function for further analysis
- **Parametersq.m**: This program defines the parameters used to diagonalize the ground state.
- **QPhase.m**: This program diagonalizes the ground state. It can easily be modified to produce the plots shown in section (4.1).

The next programs are specific for each sub-folder

TimePhase_vOne

- **Master.m**: This program runs TimeSolve.m for various models for $\eta(t)$ and plots $\langle \hat{J}_z \rangle$ against $\eta(t)$ for each model

TimePhase_vTwo

- **MasterEps.m**: This program runs TimeSolve.m for various models of $\eta(t)$ and ratios λ/δ. It calculates the deviation ϵ_m from the ground state and plots the results.

TimePhase_vThree

- **MasterUni.m**: This program runs TimeSolve.m for various models of $\eta(t)$ and ratios λ/δ and calculates the second derivative of $\hat{J}_z$. It also find the optimal slope for a given λ/δ and plots this slope against the second derivative, to test the universality of the phase transition

A Detailed calculations for the two-ion Boulder model

The interaction Hamiltonian for the Boulder model with two ions has the form:

$$\left.\begin{aligned}\hat{H}_I = &|0\rangle\langle e|\left(e^{i\overline{k}_1\hat{\overline{r}}_1}\alpha_{10}e^{-i\omega_1 t}+e^{i\overline{k}_2\hat{\overline{r}}_1}\alpha_{20}e^{-i\omega_2 t}+e^{i\overline{k}_1\hat{\overline{r}}_2}\alpha_{10}e^{-i\omega_1 t}+e^{i\overline{k}_2\hat{\overline{r}}_2}\alpha_{20}e^{-i\omega_2 t}\right)+H.C.\\ &+|1\rangle\langle e|\left(e^{i\overline{k}_1\hat{\overline{r}}_1}\alpha_{11}e^{-i\omega_3 t}+e^{i\overline{k}_2\hat{\overline{r}}_1}\alpha_{21}e^{-i\omega_4 t}+e^{i\overline{k}_1\hat{\overline{r}}_2}\alpha_{11}e^{-i\omega_3 t}+e^{i\overline{k}_2\hat{\overline{r}}_2}\alpha_{21}e^{-i\omega_4 t}\right)+H.C.+\Delta|e\rangle\langle e|\end{aligned}\right\} \tag{65}$$

where $\alpha_{ij}=\Omega_i\alpha'_{i,j}=D^{\pm}E_0/2\alpha'_{ij}$. We expand the state $|\psi\rangle$ of the system in terms of the eigenstates of the interaction-free Hamiltonian:

$$|\psi\rangle = c_0|0\rangle + c_1|1\rangle + c_e|e\rangle \tag{66}$$

The Schrödinger equation $i\frac{\mathrm{d}\psi}{\mathrm{d}t}=\hat{H}_I|\psi\rangle$ gives a set of differential equations describing the time evolution of the coefficients:

$$i\dot{c}_0 = c_e\left(e^{i\overline{k}_1\hat{\overline{r}}_1}\alpha_{10}e^{-i\omega_1 t}+e^{i\overline{k}_2\hat{\overline{r}}_1}\alpha_{20}e^{-i\omega_2 t}+e^{i\overline{k}_1\hat{\overline{r}}_2}\alpha_{10}e^{-i\omega_1 t}+e^{i\overline{k}_2\hat{\overline{r}}_2}\alpha_{20}e^{-i\omega_2 t}\right) \tag{67}$$

$$i\dot{c}_1 = c_e\left(e^{i\overline{k}_1\hat{\overline{r}}_1}\alpha_{11}e^{-i\omega_3 t}+e^{i\overline{k}_2\hat{\overline{r}}_1}\alpha_{21}e^{-i\omega_4 t}+e^{i\overline{k}_1\hat{\overline{r}}_2}\alpha_{11}e^{-i\omega_3 t}+e^{i\overline{k}_2\hat{\overline{r}}_2}\alpha_{21}e^{-i\omega_4 t}\right) \tag{68}$$

$$\left.\begin{aligned}i\dot{c}_e = &c_0\left(e^{-i\overline{k}_1\hat{\overline{r}}_1}\alpha_{10}e^{i\omega_1 t}+e^{-i\overline{k}_2\hat{\overline{r}}_1}\alpha_{20}e^{i\omega_2 t}+e^{-i\overline{k}_1\hat{\overline{r}}_2}\alpha_{10}e^{i\omega_1 t}+e^{-i\overline{k}_2\hat{\overline{r}}_2}\alpha_{20}e^{i\omega_2 t}\right)\\ &+c_1\left(e^{-i\overline{k}_1\hat{\overline{r}}_1}\alpha_{11}e^{i\omega_3 t}+e^{-i\overline{k}_2\hat{\overline{r}}_1}\alpha_{21}e^{i\omega_4 t}+e^{-i\overline{k}_1\hat{\overline{r}}_2}\alpha_{11}e^{i\omega_3 t}+e^{-i\overline{k}_2\hat{\overline{r}}_2}\alpha_{21}e^{i\omega_4 t}\right)+c_e\Delta\end{aligned}\right\} \tag{69}$$

We adiabatically eliminate the third energy level by setting $\dot{c}_e=0$, which gives e expression for c_e:

$$c_e = \left\{\begin{array}{l} -\frac{c_0}{\Delta}\left(e^{-i\overline{k}_1\hat{\overline{r}}_1}\alpha_{10}e^{i\omega_1 t}+e^{-i\overline{k}_2\hat{\overline{r}}_1}\alpha_{20}e^{i\omega_2 t}+e^{-i\overline{k}_1\hat{\overline{r}}_2}\alpha_{10}e^{i\omega_1 t}+e^{-i\overline{k}_2\hat{\overline{r}}_2}\alpha_{20}e^{i\omega_2 t}\right)\\ +-\frac{c_1}{\Delta}\left(e^{-i\overline{k}_1\hat{\overline{r}}_1}\alpha_{11}e^{i\omega_3 t}+e^{-i\overline{k}_2\hat{\overline{r}}_1}\alpha_{21}e^{i\omega_4 t}+e^{-i\overline{k}_1\hat{\overline{r}}_2}\alpha_{11}e^{i\omega_3 t}+e^{-i\overline{k}_2\hat{\overline{r}}_2}\alpha_{21}e^{i\omega_4 t}\right)\end{array}\right\} \tag{70}$$

which, by substituting into equations (67) and (68) yields the following set of differential equations:

$$i\dot{c}_0 = \left\{\begin{array}{l} -\frac{c_0}{\Delta}\left[\begin{array}{l}\alpha_{10}^2\left(2+e^{i\overline{k}_1\hat{\overline{d}}}+e^{-i\overline{k}_1\overline{d}}\right)+\alpha_{20}^2\left(2+e^{i\overline{k}_2\overline{d}}+e^{-i\overline{k}_2\hat{\overline{d}}}\right)\\ \alpha_{10}\alpha_{20}e^{i(\omega_2-\omega_1)t}\left[e^{i\Delta\overline{k}\hat{\overline{r}}_1}+e^{i\Delta\overline{k}\hat{\overline{r}}_2}+e^{i\left(\overline{k}_1\hat{\overline{r}}_1-\overline{k}_2\hat{\overline{r}}_2\right)}+e^{i\left(\overline{k}_1\hat{\overline{r}}_2-\overline{k}_2\hat{\overline{r}}_1\right)}+C.C.\right]\end{array}\right]\\ -\frac{c_1}{\Delta}\left[\begin{array}{l}\alpha_{10}\alpha_{11}e^{i(\omega_3-\omega_1)t}\left(2+e^{i\overline{k}_1\hat{\overline{d}}}+e^{-i\overline{k}_1\hat{\overline{d}}}\right)+\alpha_{20}\alpha_{21}e^{i(\omega_4-\omega_2)t}\left(2+e^{i\overline{k}_2\hat{\overline{d}}}+e^{-i\overline{k}_2\hat{\overline{d}}}\right)\\ \alpha_{20}\alpha_{11}e^{i(\omega_3-\omega_2)}\left[e^{-i\Delta\overline{k}\hat{\overline{r}}_1}+e^{-i\Delta\overline{k}\hat{\overline{r}}_2}+e^{i\left(\overline{k}_2\hat{\overline{r}}_2-\overline{k}_1\hat{\overline{r}}_1\right)}+e^{i\left(\overline{k}_2\hat{\overline{r}}_1-\overline{k}_1\hat{\overline{r}}_2\right)}\right]\\ \alpha_{10}\alpha_{21}e^{i(\omega_4-\omega_1)}\left[e^{i\Delta\overline{k}\hat{\overline{r}}_2}+e^{i\Delta\overline{k}\hat{\overline{r}}_1}+e^{i\left(\overline{k}_1\hat{\overline{r}}_1-\overline{k}_2\hat{\overline{r}}_2\right)}+e^{i\left(\overline{k}_1\hat{\overline{r}}_2-\overline{k}_2\hat{\overline{r}}_1\right)}\right]\end{array}\right]\end{array}\right\} \tag{71}$$

$$i\dot{c}_1 = \left\{\begin{array}{l} -\frac{c_0}{\Delta}\left[\begin{array}{l}\alpha_{10}\alpha_{11}e^{i(\omega_1-\omega_3)t}\left(2+e^{i\overline{k}_1\hat{\overline{d}}}+e^{-i\overline{k}_1\hat{\overline{d}}}\right)+\alpha_{20}\alpha_{21}e^{i(\omega_2-\omega_4)t}\left(2+e^{i\overline{k}_2\hat{\overline{d}}}+e^{-i\overline{k}_2\hat{\overline{d}}}\right)\\ \alpha_{20}\alpha_{11}e^{i(\omega_2-\omega_3)}\left[e^{i\Delta\overline{k}\hat{\overline{r}}_1}+e^{i\Delta\overline{k}\hat{\overline{r}}_2}+e^{i\left(\overline{k}_1\hat{\overline{r}}_1-\overline{k}_2\hat{\overline{r}}_2\right)}+e^{i\left(\overline{k}_1\hat{\overline{r}}_2-\overline{k}_2\hat{\overline{r}}_1\right)}\right]\\ \alpha_{10}\alpha_{21}e^{i(\omega_1-\omega_4)}\left[e^{-i\Delta\overline{k}\hat{\overline{r}}_2}+e^{-i\Delta\overline{k}\hat{\overline{r}}_1}+e^{i\left(\overline{k}_2\hat{\overline{r}}_2-\overline{k}_1\hat{\overline{r}}_1\right)}+e^{i\left(\overline{k}_2\hat{\overline{r}}_1-\overline{k}_1\hat{\overline{r}}_2\right)}\right]\end{array}\right]\\ -\frac{c_1}{\Delta}\left[\begin{array}{l}\alpha_{11}^2\left(2+e^{i\overline{k}_1\hat{\overline{d}}}+e^{-i\overline{k}_1\overline{d}}\right)+\alpha_{21}^2\left(2+e^{i\overline{k}_2\hat{\overline{d}}}+e^{-i\overline{k}_2\overline{d}}\right)\\ \alpha_{11}\alpha_{21}e^{i(\omega_3-\omega_4)t}\left[e^{i\Delta\overline{k}\hat{\overline{r}}_1}+e^{i\Delta\overline{k}\hat{\overline{r}}_2}+e^{i\left(\overline{k}_1\hat{\overline{r}}_1-\overline{k}_2\hat{\overline{r}}_2\right)}+e^{i\left(\overline{k}_1\hat{\overline{r}}_2-\overline{k}_2\hat{\overline{r}}_1\right)}+C.C.\right]\end{array}\right]\end{array}\right\} \tag{72}$$

We tune the lasers such that:

$$\begin{aligned}
\omega_1 - \omega_2 &= \delta - \nu = \omega_3 - \omega_4 \\
\omega_3 - \omega_1 &= -\omega_0 = \omega_4 - \omega_2 \\
\omega_3 - \omega_2 &= \delta - \omega_0 - \nu \\
\omega_4 - \omega_1 &= \nu - \omega_0 - \delta
\end{aligned}$$

We know from atomic physics that $\alpha_{10}\alpha_{20} = -\alpha_{11}\alpha_{21}$ and $\alpha_{20}\alpha_{11} = \alpha_{10}\alpha_{21}$. The lasers are directed at right angels, so we have that $\overline{k}_1 \perp \hat{\overline{r}}_2$ and $\overline{k}_2 \perp \hat{\overline{r}}_1$ and assume that $\overline{k}_1 \cdot \hat{\overline{r}}_1 \sim \overline{k}_2 \cdot \hat{\overline{r}}_2$, such that $e^{i\left(\overline{k}_1\hat{\overline{r}}_1 - \overline{k}_2\hat{\overline{r}}_2\right)} + e^{i\left(\overline{k}_1\hat{\overline{r}}_2 - \overline{k}_2\hat{\overline{r}}_1\right)} \simeq 2$. We can write equations (71) and (72) in matrix form:

$$i\begin{pmatrix}\dot{c}_0 \\ \dot{c}_1\end{pmatrix} = \left(\hat{H}_I + \hat{H}_z\right)\begin{pmatrix}c_0 \\ c_1\end{pmatrix} \tag{73}$$

This splitting of the Hamiltonian into two parts will become clear later. This enables us to write the Hamiltonians in terms of $\hat{\sigma}_z, \hat{\sigma}_+$ and $\hat{\sigma}_-$:

$$\begin{aligned}
\hat{H}_I =& \frac{\alpha'_{10}\alpha'_{20}E_0^2 D^- D^+}{4\Delta}\hat{\sigma}_z\left[e^{i(\nu-\delta)t}\left(e^{-i\Delta\overline{k}\hat{\overline{r}}_1} + e^{-i\Delta\overline{k}\hat{\overline{r}}_2}\right) + e^{-i(\nu-\delta)t}\left(e^{i\Delta\overline{k}\hat{\overline{r}}_1} + e^{i\Delta\overline{k}\hat{\overline{r}}_2}\right)\right] \\
&+ \left(\frac{\alpha'_{10}\alpha'_{11}E_0^2 D^- D^+}{4\Delta}\hat{\sigma}_+ e^{-i\omega_0 t}\left[e^{i\overline{k}_1\hat{\overline{d}}} + e^{-i\overline{k}_1\hat{\overline{d}}} + e^{i\overline{k}_2\hat{\overline{d}}} + e^{-i\overline{k}_2\hat{\overline{d}}}\right] + H.C.\right)
\end{aligned}$$

$$\begin{aligned}
\hat{H}_z =& -\frac{c_0}{\Delta}\left[\alpha_{10}^2\left(2 + e^{i\overline{k}_1\overline{d}} + e^{-i\overline{k}_1\overline{d}}\right) + \alpha_{20}^2\left(2 + e^{i\overline{k}_2\overline{d}} + e^{-i\overline{k}_2\overline{d}}\right)\right]|0\rangle\langle 0| \\
&- \frac{c_1}{\Delta}\left[\alpha_{11}^2\left(2 + e^{i\overline{k}_1\overline{d}} + e^{-i\overline{k}_1\overline{d}}\right) + \alpha_{22}^2\left(2 + e^{i\overline{k}_2\overline{d}} + e^{-i\overline{k}_2\overline{d}}\right)\right]|1\rangle\langle 1| \\
&+ \left(\frac{\Omega_x}{2}\hat{\sigma}_+\left\{e^{i(\delta-\omega_0-\nu)t}\left[2 + e^{-i\Delta\overline{k}\hat{\overline{r}}_1} + e^{-i\Delta\overline{k}\hat{\overline{r}}_2}\right] + e^{i(\nu-\omega_0-\delta)t}\left[2 + e^{i\Delta\overline{k}\hat{\overline{r}}_1} + e^{i\Delta\overline{k}\hat{\overline{r}}_2}\right]\right\} + H.C.\right)
\end{aligned}$$

where the expressions for α_{ij} have been inserted into $\hat{H}_I$. The Rabi frequencies are defined as

$$\Omega_p \equiv \frac{\alpha'_{10}\alpha'_{20}E_0^2 D^- D^+}{2\Delta} \tag{74}$$

$$\Omega_x \equiv \frac{\alpha'_{10}\alpha'_{11}E_0^2 D^- D^+}{\Delta} \tag{75}$$

We need to consider the spatial exponential functions before we change to the interaction picture, where $\hat{\overline{r}}_i = \overline{r}_{0,i} + \delta\hat{\overline{r}}$. We have, for the $\hat{\sigma}_z$ term:

$$\begin{aligned}
e^{i\Delta\overline{k}\delta\hat{\overline{r}}}\left[e^{i\Delta\overline{k}\hat{\overline{r}}_{0,1}} + e^{i\Delta\overline{k}\hat{\overline{r}}_{0,2}}\right] &= e^{i\Delta\overline{k}\delta\hat{\overline{r}}}e^{i\Delta\overline{k}\frac{\hat{\overline{r}}_{0,1}+\hat{\overline{r}}_{0,2}}{2}}\left(e^{i\Delta\overline{k}\frac{\hat{\overline{r}}_{0,1}-\hat{\overline{r}}_{0,2}}{2}} + e^{i\Delta\overline{k}\frac{-\hat{\overline{r}}_{0,1}+\hat{\overline{r}}_{0,2}}{2}}\right) \\
&= 2e^{i\Delta\overline{k}\delta\hat{\overline{r}}}e^{i\Delta\overline{k}\frac{\hat{\overline{r}}_{0,1}+\hat{\overline{r}}_{0,2}}{2}}\cos\left(\Delta\overline{k}\frac{\hat{\overline{r}}_{0,1} - \hat{\overline{r}}_{0,2}}{2}\right) \\
&= 2e^{i\Delta\overline{k}\delta\hat{\overline{r}}}e^{i\Delta\overline{k}\frac{\hat{\overline{r}}_{0,1}+\hat{\overline{r}}_{0,2}}{2}}\cos\left(\frac{\Delta\overline{k}\ \hat{\overline{d}}}{2}\right)
\end{aligned}$$

We see from the cosine-part that constructive interference occurs when

$$\overline{k}\ \hat{\overline{d}} = 2\pi p, \quad p \in \mathbb{Z} \tag{76}$$

which also ensures that $e^{i\Delta\overline{k}\frac{\hat{\overline{r}}_{0,1}+\hat{\overline{r}}_{0,2}}{2}} = 1$ due to the periodicity of the potential. We have for the $\hat{\sigma}_+$ term:

$$\begin{aligned}
e^{\pm i\overline{k}_1\hat{\overline{d}}} + e^{\pm i\overline{k}_2\hat{\overline{d}}} &= e^{\pm i\hat{\overline{d}}\left(\overline{k}_1 - \overline{k}_2\right)}\left(e^{\pm i\Delta\overline{k}\ \hat{\overline{d}}} + e^{\mp i\Delta\overline{k}\ \hat{\overline{d}}}\right) \\
&= 2e^{i\hat{\overline{d}}\left(\overline{k}_1 - \overline{k}_2\right)}\cos\left(\frac{\overline{k}\ \hat{\overline{d}}}{2}\right)
\end{aligned} \tag{77}$$

where this term has the same requirement for constructive interference, $\overline{k}\ \hat{\overline{d}} = 2\pi p$. This also ensures that $e^{i\hat{\overline{d}}(\overline{k}_1 - \overline{k}_2)} = 1$.
This gives the effective interaction Hamiltonian:

$$\hat{H}_I = \Omega_p \hat{\sigma}_z \left[e^{i(\nu-\delta)t} e^{-i\Delta\overline{k}\delta\hat{\overline{r}}} + e^{-i(\delta-\nu)t} e^{i\Delta\overline{k}\delta\hat{\overline{r}}} \right] + \left(\Omega_x e^{i\Delta\overline{k}\delta\hat{\overline{r}}} \hat{\sigma}_+ e^{-i\omega_0 t} + H.C. \right) \tag{78}$$

We can rewrite this Hamiltonian by using $e^{\pm i\Delta\overline{k}\delta\hat{\overline{r}}} \approx 1 \pm i\eta \left(\hat{a} + \hat{a}^\dagger \right)$ and $2i \sin x = e^{ix} - e^{-ix}$. This gives:

$$\hat{H}_I = \frac{\Omega_x}{2} \left[\hat{\sigma}_+ e^{-i\omega_0 t} + H.C. \right] - 2\Omega_p \hat{\sigma}_z \left(\hat{a} + \hat{a}^\dagger \right) \sin\left([\nu - \delta] t \right) \tag{79}$$

We change to the interaction picture with respect to $\hat{H}_0 = \frac{\omega_0}{2}\hat{\sigma}_z + (\nu - \delta)\, \hat{a}^\dagger \hat{a}$ using standard quantum optics methods. This yields:

$$\hat{H}_I \approx \delta \hat{a}^\dagger \hat{a} + \frac{\Omega_x}{2} \sigma_x + \eta \Omega_p i \hat{\sigma}_z \left(\hat{a} - \hat{a}^\dagger \right) \tag{80}$$

There is a extra term in equation (78) of the form $2\cos\left([\nu - \delta] t \right)$ which is approximately zero when we change to the interaction picture.
It can be shown, using similar methods, that $\hat{H}_z \approx 0$ when we change to the interaction picture and such will not contribute to the dynamics of the system.

B Detailed Holstein-Primakoff Transformations

The phase transition for the Hamiltonian for the Innsbruck model, given by equation (25), can be described by expressing the atomic angular momentum operators as in terms of creation $\hat{b}$ and annihilation $\hat{b}^\dagger$ operators of a second mode of light through the Holstein-Primakoff transformations:

$$\hat{J}_+ = \hat{b}^\dagger \sqrt{2J - \hat{b}^\dagger \hat{b}} \tag{81}$$

$$\hat{J}_- = \sqrt{2J - \hat{b}^\dagger \hat{b}}\, \hat{b} \tag{82}$$

$$\hat{J}_z = \hat{b}^\dagger \hat{b} - J \tag{83}$$

The Hamiltonian is in this representation:

$$\hat{H} = \lambda \left(\hat{b}^\dagger \hat{b} - j \right) + \delta \hat{a}^\dagger \hat{a} + \eta' \left(\hat{a} + \hat{a}^\dagger \right) \left(\hat{b}^\dagger \sqrt{1 - \frac{\hat{b}^\dagger \hat{b}}{2J}} + \sqrt{1 - \frac{\hat{b}^\dagger \hat{b}}{2J}}\, \hat{b} \right) \tag{84}$$

where $\lambda = \epsilon_0/2$ and $\eta' = \eta/2$. The parity operator, given by equation (26) is:

$$\Pi = \exp\left[i\pi \left(\hat{a}^\dagger \hat{a} + \hat{b}^\dagger \hat{b} \right) \right] \tag{85}$$

The Normal Phase

The normal phase can be described by neglecting terms with j in the denominator in equation (84). This gives

$$\hat{H} = \lambda \hat{b}^\dagger \hat{b} + \delta \hat{a}^\dagger \hat{a} + \eta' \left(\hat{a} + \hat{a}^\dagger \right) \left(\hat{b} + \hat{b}^\dagger \right) - J\lambda \tag{86}$$

The description is made clearer by introducing position and momentum operators for the two modes:

$$\hat{x} = \frac{1}{\sqrt{2\delta}} \left(\hat{a} + \hat{a}^\dagger \right), \qquad \hat{p}_x = i\sqrt{\frac{\delta}{2}} \left(\hat{a}^\dagger - \hat{a} \right) \tag{87}$$

$$\hat{y} = \frac{1}{\sqrt{2\lambda}} \left(\hat{b} + \hat{b}^\dagger \right), \qquad \hat{p}_y = i\sqrt{\frac{\lambda}{2}} \left(\hat{b}^\dagger - \hat{b} \right) \tag{88}$$

The Hamiltonian can then be written as:

$$\hat{H} = \frac{1}{2}\left[\delta^2 x^2 + p_x^2 + \lambda^2 y^2 + p_y^2 + 4\eta'\sqrt{\delta\lambda}xy - \delta - \lambda\right] - J\lambda \tag{89}$$

This Hamiltonian has the form of two harmonic oscillators in $x-$ and $y-$coordinates that are coupled together by the term $4\eta\sqrt{\delta\lambda}xy$. This Hamiltonian can be written in diagonal form by rotating the coordinate frame according to:

$$\begin{pmatrix} q_1 \\ q_2 \end{pmatrix} = \begin{pmatrix} \cos\gamma^{(1)} & \sin\gamma^{(1)} \\ -\sin\gamma^{(1)} & \cos\gamma^{(1)} \end{pmatrix} \begin{pmatrix} x \\ y \end{pmatrix} \tag{90}$$

where the angle $\gamma^{(1)}$ is defined as

$$\tan 2\gamma^{(1)} = \frac{4\eta'\sqrt{\delta\lambda}}{\lambda^2 - \delta^2} \tag{91}$$

$$\gamma^{(1)} \to \frac{\pi}{4} \quad \text{for} \quad \delta \to \lambda \tag{92}$$

This is found by setting the equations in (90) equation (89) and setting the coefficient for the non-linear term equal to zero. Using the limit in equation (92), we have

$$x = \frac{1}{\sqrt{2}}(q_1 + q_2) \tag{93}$$

$$y = \frac{1}{\sqrt{2}}(-q_1 + q_2) \tag{94}$$

The Hamiltonian can then be written as:

$$\hat{H} = \frac{1}{2}\left[\delta^2 q_1^2 + p_1^2 + \lambda^2 q_2^2 + p_2^2 + 4\eta'\sqrt{\delta\lambda}\left(q_2^2 - q_1^2\right) + \left(\delta^2 - \lambda^2\right)q_1 q_2\right] + \frac{1}{2}(-\delta - \lambda) + J\lambda \tag{95}$$

We can write the position-dependant part in matrix form by:

$$\hat{H}_Q = \begin{pmatrix} q_1 & q_2 \end{pmatrix} \begin{pmatrix} A & B \\ C & D \end{pmatrix} \begin{pmatrix} q_1 \\ q_2 \end{pmatrix} \tag{96}$$

where

$$A = \delta^2 + \lambda^2 - 4\eta\sqrt{\lambda\delta}, \qquad B = \frac{1}{2}\left(\delta^2 - \lambda^2\right) \tag{97}$$

$$D = \delta^2 + \lambda^2 + 4\eta\sqrt{\lambda\delta}, \qquad C = \frac{1}{2}\left(\delta^2 - \lambda^2\right) \tag{98}$$

This can be diagonalized in the usual way. The results are:

$$\epsilon_{\pm}^{(1)^2} = \frac{1}{2}\left[\delta^2 + \lambda^2 \pm \sqrt{\left(\lambda^2 - \delta^2\right)^2 + 16\eta'^2\delta\lambda}\right] \tag{99}$$

The energies need to be real, so we need

$$\delta^2 + \lambda^2 > \sqrt{\left(\lambda^2 - \delta^2\right)^2 + 16\eta'^2\delta\lambda} \tag{100}$$

$$\Rightarrow \eta' < \frac{\sqrt{\lambda\delta}}{2} \Rightarrow \eta < \sqrt{\lambda/\delta} \tag{101}$$

and the Hamiltonian takes the form

$$\hat{H} = \frac{1}{2}\left[\epsilon_{-}^{(1)^2} q_1^2 + p_1^2 + \epsilon_{+}^{(1)^2} q_2^2 + p_2^2 - \delta^2 - \lambda^2\right] - J\lambda \tag{102}$$

which has the form of two uncoupled harmonic oscillators. The Hamiltonian can be written in terms of two new bosonic modes, corresponding to the rotated coordinates:

$$q_1 = \sqrt{\frac{1}{2\epsilon_-^{(1)}}}\left(\hat{c}_1 + \hat{c}_1^\dagger\right), \qquad p_1 = i\sqrt{\frac{\epsilon_-^{(1)}}{2}}\left(\hat{c}_1^\dagger - \hat{c}_1\right) \tag{103}$$

$$q_2 = \sqrt{\frac{1}{2\epsilon_+^{(1)}}}\left(\hat{c}_2 + \hat{c}_2^\dagger\right), \qquad p_2 = i\sqrt{\frac{\epsilon_+^{(1)}}{2}}\left(\hat{c}_2^\dagger - \hat{c}_2\right) \tag{104}$$

which yields the Hamiltonian

$$\hat{H} = \epsilon_-^{(1)}\hat{c}_1^\dagger\hat{c}_1 + \epsilon_+^{(1)}\hat{c}_2^\dagger\hat{c}_2 + \frac{1}{2}\left(\epsilon_-^{(1)} + \epsilon_-^{(2)} - \delta - \lambda\right) - \lambda J \tag{105}$$

The Excited Phase

A mean field description to first order can be made by modifying the bosonic modes to have macroscopic displacements, corresponding to the macroscopic excitations shown in section (4.1):

$$\hat{a} \to \hat{c} \pm \sqrt{\alpha}, \quad \hat{b} \to \hat{d} \mp \sqrt{\beta} \tag{106}$$

where the choice of sign is arbitrary, except for a few changes of sign in the following. The Hamiltonian becomes:

$$\left.\begin{aligned}\hat{H} =& \lambda\left[\hat{d}^\dagger\hat{d} - \sqrt{\beta}\left(\hat{d} + \hat{d}\right) + \beta - j\right] + \delta\left[\hat{c}^\dagger\hat{c} + \sqrt{\alpha}\left(\hat{c} + \hat{c}^\dagger\right) + \alpha\right] \\ &+ \eta'\sqrt{\frac{2j-\beta}{2j}}\left[\hat{c} + \hat{c}^\dagger + 2\sqrt{\alpha}\right]\left[\hat{d}^\dagger K + K\hat{d} - 2\sqrt{\beta}K\right]\end{aligned}\right\} \tag{107}$$

where

$$K = \sqrt{1 - \frac{\hat{d}^\dagger\hat{d} - \sqrt{\beta}\left(\hat{d} + \hat{d}^\dagger\right)}{2j - \beta}} \simeq 1 - \frac{\hat{d}^\dagger\hat{d} - \sqrt{\beta}\left(\hat{d} + \hat{d}^\dagger\right)}{2\left(2j - \beta\right)}$$

The first-order mean field description is done by expanding K to first order. This yields:

$$\begin{aligned}\hat{H} =& \delta\hat{c}^\dagger\hat{c} + \left[\lambda + \frac{2\eta'}{k}\sqrt{\frac{k\alpha\beta}{2j}}\left(j - \beta\right)\right]\hat{d}^\dagger\hat{d} - \left[2\eta'\sqrt{\frac{\beta}{2j}} - \delta\sqrt{\alpha}\right]\left(\hat{c} + \hat{c}^\dagger\right) \\ &\left[-\lambda\sqrt{\beta} + \frac{4\eta'}{k}\sqrt{\frac{\alpha k}{2j}}\left(j - \beta\right)\right]\left(\hat{d} + \hat{d}^\dagger\right)^2 + \frac{\eta'}{2k^2}\sqrt{\frac{\alpha\beta k}{2j}}\left(2k + \beta\right)\left(\hat{d} + \hat{d}^\dagger\right)^2 \\ &+ \frac{2\eta'}{k}\sqrt{\frac{k}{2j}}\left(j - \beta\right)\left(\hat{c} + \hat{c}\dagger\right)\left(\hat{d} + \hat{d}\dagger\right) + \left[\lambda\left(\beta - j\right) + \delta\alpha - \frac{\eta'}{\lambda}\sqrt{\frac{\alpha\beta k}{2j}}\left(1 + 4k\right)\right]\end{aligned}$$

The terms that are linear in the bosonic operators can be eliminated by choosing

$$\sqrt{\alpha} = \frac{2\eta'}{\delta}\sqrt{\frac{j}{2}\left(1 - \mu^2\right)} \tag{108}$$

$$\sqrt{\beta} = \sqrt{j\left(1 - \mu\right)} \tag{109}$$

where $\mu = \frac{\delta\lambda}{4\eta'^2}$. Rearranging some of the other terms gives another form of the Hamiltonian:

$$\begin{aligned}\hat{H} =& \delta\hat{c}^\dagger\hat{c} + \frac{\lambda}{2\mu}\left(1 + \mu\right)\hat{d}^\dagger\hat{d} + \frac{\lambda\left(1 - \mu\right)\left(3 + \mu\right)}{8\mu\left(1 + \mu\right)}\left(\hat{d} + \hat{d}^\dagger\right)^2 \\ &+ \eta'\mu\sqrt{\frac{2}{1 + \mu}}\left(\hat{c} + \hat{c}^\dagger\right)\left(\hat{d} + \hat{d}\right) - j\left[\frac{2\eta'^2}{\delta} + \frac{\delta\lambda^2}{8\eta'^2}\right] - \frac{\eta'^2}{\delta}\left(1 - \mu\right)\end{aligned}$$

where we define $\tilde{\omega} \equiv \frac{\lambda}{2\mu}(1+\mu)$. We then introduce position and momentum operators:

$$\hat{X} = \frac{1}{\sqrt{2\delta}}\left(\hat{c}+\hat{c}^\dagger\right), \qquad \hat{p}_X = i\sqrt{\frac{\delta}{2}}\left(\hat{c}^\dagger - \hat{d}\right) \tag{110}$$

$$\hat{Y} = \frac{1}{\sqrt{2\tilde{\omega}}}\left(\hat{d}+\hat{d}^\dagger\right), \qquad \hat{p}_Y = i\sqrt{\frac{\tilde{\omega}}{2}}\left(\hat{d}^\dagger - \hat{d}\right) \tag{111}$$

The Hamiltonian can be diagonalized in the same manner is in the normal phase. The diagonalized Hamiltonian is:

$$\hat{H} = \epsilon_-^{(2)}\hat{e}_1^\dagger\hat{e}_1 + \epsilon_+^{(2)}\hat{e}_2^\dagger\hat{e}_2 - j\left[\frac{2\eta'^2}{\delta} + \frac{\lambda^2\delta}{8\eta'^2}\right] + \frac{1}{2}\left(\epsilon_+^{(2)} + \epsilon_-^{(2)} - \frac{\lambda}{2\mu}(1+\mu) - \delta - \frac{2\eta'^2}{\delta}(1-\mu)\right) \tag{112}$$

with oscillator energies

$$2\epsilon_\pm^{(1)} = \frac{\lambda^2}{\mu^2} + \delta^2 \pm \sqrt{\left[\frac{\lambda^2}{\mu^2} - \delta^2\right]^2 + 4\lambda^2\delta^2} \tag{113}$$

These need to be real, so we need:

$$\frac{\lambda^2}{\mu^2} + \delta^2 > \sqrt{\left[\frac{\lambda^2}{\mu^2} - \delta^2\right]^2 + 4\lambda^2\delta^2} \tag{114}$$

$$\Rightarrow \eta > \sqrt{\lambda\delta} \tag{115}$$

and where $\hat{e}_1$ and $\hat{e}_2$ are new bosonic modes defined from the rotated coordinates.

C Phonon Harmonic Oscillator

Consider N ions that are kept in an one-dimensional ion trap. An ion will oscillate if it interacts with a light field. This causes the other ions to oscillate in response. This response is modelled as an harmonic oscillator, where we assume that each ion is connected by a spring of length L with spring constant C. The displacement of the $j'th$ particle is x_j and the momentum is p_j. The Hamiltonian is:

$$\hat{H} = \frac{1}{2}\sum_{j=1}^{N}\left[\frac{1}{M}p_j^2 + C\left(x_{j+1} - x_j\right)^2\right] \tag{116}$$

We assume that the ions are subject to the periodic boundary condition $x_j = x_{j+N}$. This Hamiltonian can be significantly simplified by changing to phonon coordinates by taking the Fourier transform of x_j and p_j. The Fourier transform q_k of x_j is:

$$q_k = N^{-1/2}\sum_{j=1}^{N} x_j e^{-ikjL} \tag{117}$$

with the inverse transformation

$$x_j = N^{-1/2}\sum_{k=1}^{N} q_k e^{ikjL} \tag{118}$$

where k is the wavevector with the N values given by the periodic boundary condition:

$$k = \frac{2\pi n}{NL}, \quad n = 0, \pm1, \pm2, ..., \pm\left(\frac{1}{2}N - 1\right), \frac{1}{2}N \tag{119}$$

The Fourier transform of the momentum need to be the canonical conjugate of x_j:

$$P_k = N^{-1/2}\sum_{j=1}^{N} p_j e^{ikjL}, \quad p_j = N^{-1/2}\sum_{k=1}^{N} P_k e^{-ikjL} \tag{120}$$

Note the opposite sign in the exponential functions, these ensures that the two transformed coordinates are canonical conjugates:

$$\begin{aligned}[q_k, P_k] &= N^{-1}\left[\sum_{l=1}^{N} x_l e^{-iklL}, \sum_{j=1}^{N} p_j e^{ik'jL}\right] \\ &= N^{-1}\sum_{l}\sum_{j}[x_l, p_j]\, e^{-i\left(kl-k'j\right)L}\end{aligned} \tag{121}$$

The operators x_l and p_j satisfy the commutation relation $[X_l, p_j] = i\delta_{l,j}$, where $\delta_{l,j}$ is the Kronecker delta function. Remember that we have set $\hbar = 1$ in this thesis. This gives:

$$[q_k, P_k] = N^{-1} i \sum_{l} e^{-i\left(k-k'\right)lL} = i\delta_{k,k'} \tag{122}$$

where we have used:

$$\sum_{l} e^{-i\left(k-k'\right)lL} = \sum_{l} e^{-i2\pi\left(n-n'\right)/N} = N\delta_{n,n'} = N\delta_{k,k'} \tag{123}$$

We can now transform the Hamiltonian by inserting the coordinate transformations. The momentum term is:

$$\begin{aligned}\sum_{j=1}^{N} p_j^2 &= N^{-1}\sum_{j=1}^{N}\sum_{k=1}^{N}\sum_{k'=1}^{N} P_k P_{k'} e^{-i\left(k+k'\right)lL} \\ &= \sum_{k}\sum_{k'} P_k P_{k'}\delta_{-k,k'} = \sum_{k} P_k P_{-k}\end{aligned} \tag{124}$$

The displacement term is:

$$\begin{aligned}\sum_{j=1}^{N}\left(x_{j+1}-x_j\right)^2 &= N^{-1}\sum_{j}\left(\sum_{k=1}^{N} q_k e^{ik(j+1)L} - \sum_{k'=1}^{N} q_{k'} e^{ikjL}\right)^2 \\ &= N^{-1}\sum_{j}\sum_{k}\sum_{k'} q_k q_{k'} e^{iklL}\left[e^{ikL}-1\right] e^{ik'lL}\left[e^{ik'L}-1\right] \\ &= N^{-1}\sum_{j=1}^{N}\sum_{k}\sum_{k'} q_k q_{k'} e^{i\left(k+k'\right)jL}\left[e^{ikL}-1\right]\left[e^{ik'L}-1\right] \qquad (125) \\ &= \sum_{j=1}^{N}\sum_{k} q_k q_{-k} e^{i(k-k)jL}\left[1+e^{i(k-k)L}-e^{ikL}-e^{-ikL}\right] \qquad (126) \\ &= 2\sum_{k} q_k q_{-k}\left(1-\cos\left(kL\right)\right) \qquad (127)\end{aligned}$$

where we have used $\sum_{k'} e^{i\left(k+k'\right)jL} = N\delta_{k,-k}$. We define the $k'th$ frequency by

$$\omega_k = \sqrt{\frac{2C}{M}}\sqrt{1-\cos\left(kL\right)} \tag{128}$$

The transformed Hamiltonian is then:

$$\hat{H} = \frac{1}{2}\sum_{k}\left[\frac{1}{M}P_k P_{k'} + M\omega_k^2 q_k q_{-k}\right] \tag{129}$$

which has the form of the harmonic oscillator Hamiltonian.

D Additional Plots

D.1 Linear Lamb-Dicke Parameter $\eta(t)$ for Additional Numbers of Ions

This section show additional plots used in the discussion in section (4.2.1), where the Scrödinger equation has been solved for different models of $\eta(t)$ for $N = 2, 4, 5$ ions in the trap for the slow models. This tests the phase transition for a time-dependent η for varying number of ions. We see that the number of ions do not significantly alter the behaviour of the phaser transition.

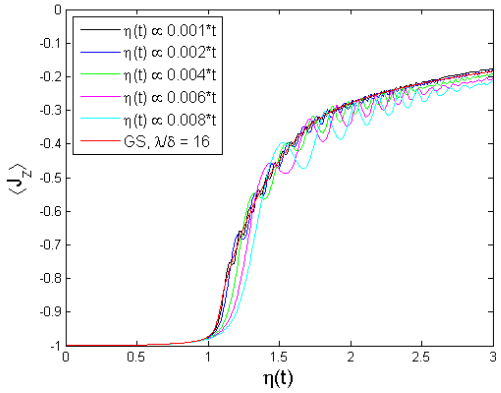

(a) Population inversion for $N = 2$ for various $\eta(t)$models

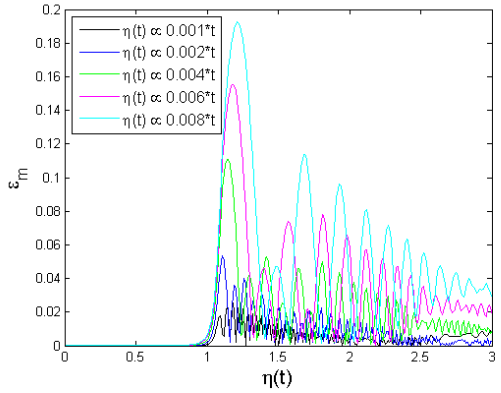

(b) The deviation from the ground state for the models

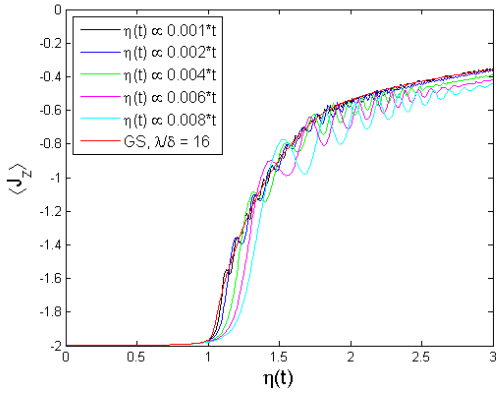

(c) Population inversion for $N = 4$ for various $\eta(t)$models

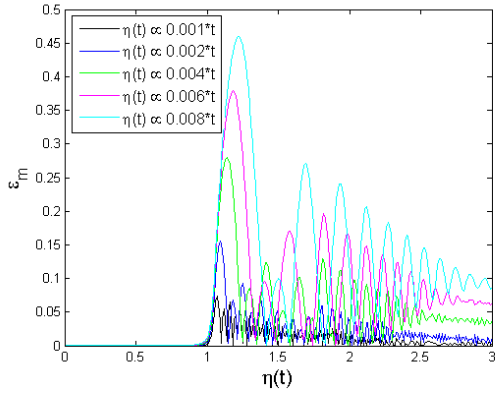

(d) The deviation from the ground state for the models

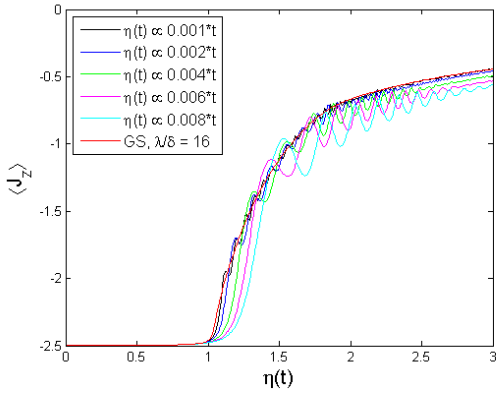

(e) Population inversion for $N = 5$ for various $\eta(t)$models

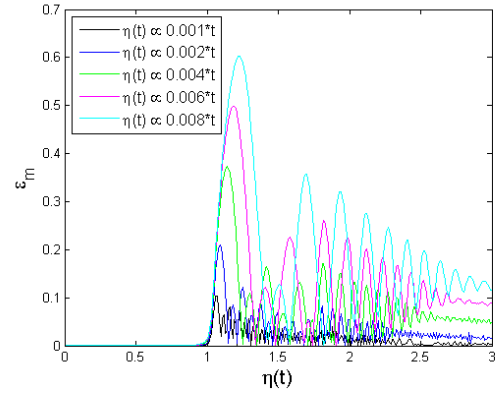

(f) The deviation from the ground state for the models

D.2 Mean Errors for Additional Numbers of Ions

The mean deviations from the ground state is shown for $N = 2, 3, 4$, as was done for $N = 3$ in section (4.2.1). It is seen the mean deviations are slightly larger for a higher number of ions, but the scaled deviation ϵ_m/N is roughly the same for all cases.

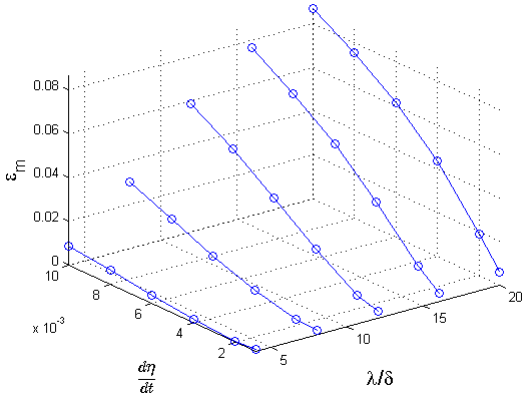

(a) Deviations for $N = 2$

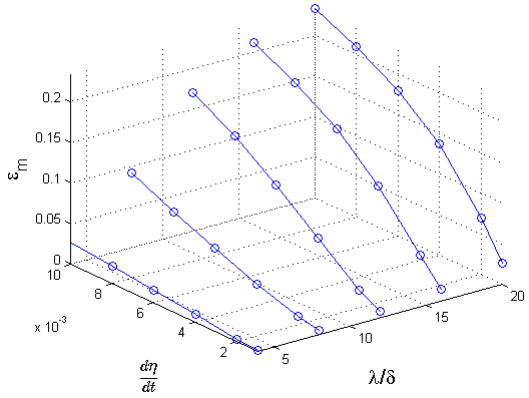

(b) Deviations for $N = 4$

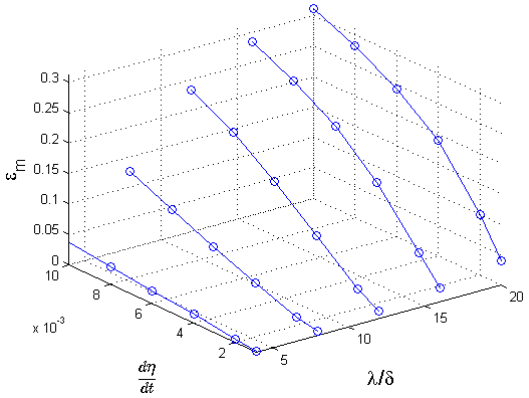

(c) Deviations for $N = 5$

Figure 8: The mean deviation from the ground state ϵ for various λ/δ and $\mathrm{d}\eta/\mathrm{d}t$

D.3 Phase Transition for the Boulder Model

The ground state of the Boulder model Hamiltonian has been diagonalized and plotted in figure (9). We see that the plot is essentially the same as for the Innsbruck model, discussed in section (4.1).

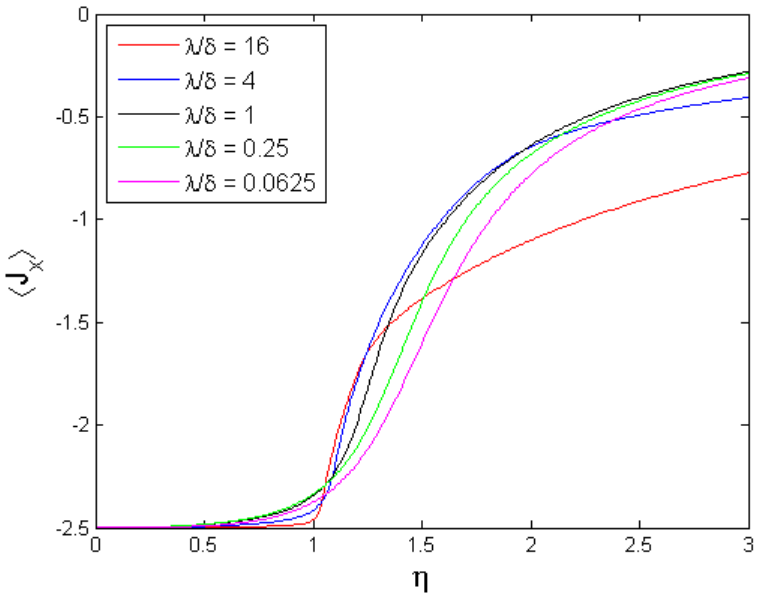

Figure 9: Expectation value of $\hat{J}_x$ for 5 ions for the Boulder Model